https://doi.org/10.5194/egusphere-2025-5972
Preprint. Discussion started: 12 December 2025

Plant hydraulic traits regulating productivity and drought resistance in boreal crops

Hui Tang[1,4], Samuli Launianen[2], Julius Vira[1], Liisa Kulmala[1,3], Taru Palosuo[2], Hermanni Aaltonen[1], Olli Nevalainen[1], Istem Fer[1], Henriikka Vekuri[1], Jari-Pekka Nousu[2], Mika Korkiakoski[1], and Jari Liski[1]

[1]Finnish Meteorological Institute (FMI), Climate System Research, Helsinki, Finland
[2]Natural Resources Institute Finland (Luke), Helsinki, Finland
[3]Institute for atmospheric and Earth system research (INAR), University of Helsinki, Finland
[4]Department of Geosciences and Geography, University of Helsinki, Finland

Correspondence: Hui Tang (hui.tang@fmi.fi)

Abstract. Crop hydraulics play a critical role in coordinating crop photosynthesis and hydraulic safety when facing water scarcity. Boreal crop hydraulic traits and their relevance to productivity and drought resistance, however, remain poorly researched. In this study, we leveraged multi-year carbon and water flux measurements from a perennial forage grass and an annual cereal (oat) field in Finland using a novel process-based model with fully-coupled plant photosynthesis, hydraulics, and soil moisture to decipher the apparent hydraulic traits of the crops and their association with crop performances under varying drought conditions. It is found that both crops exhibited remarkably low hydraulic conductance, which plays a pivotal role in preventing soil water depletion and thereby ensures a high hydraulic safety margin and productivity under drought conditions. Both crops also showed higher susceptibility to atmospheric dryness than to soil drought, likely due to their anisohydric ("risky") stomatal behaviour. The remaining discrepancy between our model-inferred hydraulic traits and available empirical data for temperate crops highlights the need for more measurements of boreal crop hydraulic traits. Our findings underscore the importance of incorporating crop hydraulic processes in process-based crop models to gain physiological insights for crop performance and to enhance their accuracy and predictive power in both current and future climates.

1 Introduction

Hydraulic traits are plant properties regulating water extraction and transport from the soil to the aerial organs, which play a fundamental role in plant productivity, notably when faced with water scarcity (Cardoso et al., 2025; Torres-Ruiz et al., 2024; Sperry and Love, 2015). More specifically, a positive correlation between photosynthetic rate and hydraulic efficiency (often interpreted as plant hydraulic conductance) has been widely observed in vascular plants (Holloway-Phillips and Brodribb, 2011a; Ocheltree et al., 2016; Gleason et al., 2021). Meanwhile, plant resistance to drought has often been linked to hydraulic safety (Choat et al., 2012; Anderegg et al., 2016), which is measured by the water potential at which a plant loses 50% of its hydraulic conductivity, underpinning the ability of plants to protect against xylem embolism and the resultant hydraulic mortality under drought stress. A trade-off between hydraulic efficiency and safety has been widely documented (Ocheltree et al., 2016; Huo et al., 2022; Zhao et al., 2025), stating that plants capable of efficiently transporting water are also more

https://doi.org/10.5194/egusphere-2025-5972
Preprint. Discussion started: 12 December 2025

vulnerable to cavitation and vice versa, primarily due to inherent structural constraints. A similar trade-off has also been found for stomatal regulation (Henry et al., 2019). However, the strength of such a trade-off is still hotly debated (Gleason et al., 2016; Sanchez-Martinez et al., 2020; Liu et al., 2021a), reflecting diverse hydraulic strategies adopted by plants to improve their fitness to variable environmental conditions.

Despite their significance, it remains elusive how hydraulic traits coordinate in boreal crops and modulate their productivity and drought response. Historically, water limitation has not been a primary concern for humid boreal agroecosystems. Therefore, hydraulic traits and drought tolerance have been less of a priority when selecting or breeding crops for the region, while other traits such as early maturity, cold tolerance, and disease resistance have received more attention (Roitsch et al., 2022). However, the situation has changed in recent years (Poque et al., 2025), as more frequent and severe drought events, characterised by limited soil water availability (soil drought) or high atmospheric evaporative demand (atmospheric drought), have been observed and are projected to occur in the future (Spinoni et al., 2018; Rantanen et al., 2023). The hydraulic traits governing the crop response to drought are expected to be under strong selective pressure in the region. Thus, a deeper understanding of the impacts of different types of drought on boreal crops and their association with crop hydraulic traits is urgently needed.

Previous studies have revealed that common crop species (mostly annual cereal crops from temperate and tropical regions) often exhibit high hydraulic conductance (efficiency) but low hydraulic safety (Holloway-Phillips and Brodribb, 2011a; Lamarque et al., 2020; Corso et al., 2020; Canales et al., 2021; Gleason et al., 2021) to obtain high crop productivity. It is thus conjectured that boreal crops, especially annual cereals (Liu et al., 2019), may hold similar acquisitive hydraulic strategy to obtain high productivity in a relatively short growing season compared to warmer climates (referred to as "efficiency hypothesis" hereafter).

On the other hand, hydraulic traits indicating high safety but low efficiency (i.e., conservative hydraulic strategy) have been observed in boreal species, mostly in trees such as pine and spruce (Li et al., 2023). Assuming the significant role of climate in shaping plant hydraulic traits of different species towards convergent adaptation (Liu et al., 2024; Wang et al., 2025), it is plausible that boreal crops can also adopt a conservative hydraulic strategy similar to other boreal species, prioritising hydraulic safety over efficiency and productivity (referred to as "safety hypothesis" hereafter). This trend may be particularly pronounced in perennial crops, known for their conservative hydraulic strategy to survive harsh winters and tolerate more stress (Vico and Brunsell, 2018; Liu et al., 2019).

Alternatively, plant hydraulic traits have been found to show phenotypical plasticity when grown under different conditions (Pritzkow et al., 2020; Sun et al., 2021; Ramírez-Valiente et al., 2025) and vary across growing stages (Yao et al., 2021), even though they are commonly regarded as inherent and conserved features within each species (Lamy et al., 2014). Given the strong seasonality of the boreal climate, we posit that the hydraulic traits of boreal crops can exhibit plasticity at different phenological stages and acclimation to varying growing conditions (referred to as "plasticity hypothesis"). This would allow crops to optimise both productivity and drought resistance across their life cycle.

To test the above competing hypotheses for boreal crops, we leveraged multi-year observation of carbon and water fluxes from two crop fields in Finland by utilizing a novel process-based model with explicit depiction of plant hydraulics coupled

https://doi.org/10.5194/egusphere-2025-5972
Preprint. Discussion started: 12 December 2025

with photosynthesis and soil moisture dynamics. We deciphered the hydraulic traits of the crops and their association with crop performance such as productivity, water use efficiencies, and drought responses. The two crop fields were covered with a perennial crop (forage grass) and an annual crop (oat), respectively. This allows us to examine not only the hydraulic traits of contrasting crop types but also the plasticity of these traits under different growing conditions.

Process-based models with an explicit representation of plant hydraulic processes have emerged only recently and have been shown to better describe plant responses to drought, especially atmospheric drought, than models without hydraulic processes (Kennedy et al., 2019; Liu et al., 2020). They are also shown to be valuable tools for revealing plant's hydraulic traits (so called model inversion) (Wang et al., 2020; Gleason et al., 2022; Liu et al., 2021b; Lu et al., 2022). In particular, the use of field-level flux measurements to constrain the hydraulic parameters of such models has been proven effective in retrieving plant's apparent hydraulic traits (Liu et al., 2020). Here, "apparent" means an average of the hydraulic traits over collective individuals of the same or different species at a field or ecosystem level, which is in contrast to the hydraulic traits measured for individual plants in laboratory and gardening studies.

In the following sections, we first outline the framework of the newly developed process-based model SPY-C, the study sites and observation data, and the workflow of the model inversion to deduce the apparent hydraulic traits. We then illustrate the hydraulic traits inferred for the boreal crops and their impact on crop productivity and drought response. How these findings support our hypotheses and the remaining issues for future studies are discussed in the end.

2 Materials and Methods

2.1 Structure of SPY-C

We developed a comprehensive soil-plant-atmosphere model SPY-C, illustrated in Fig. 1. The model is composed of four interlinked modules mostly from existing models: plant photosynthesis and hydraulics (Phydro), soil water balance (SpaFHy), soil organic carbon decomposition (Yasso), and a simple data-driven phenology and allocation module (PA). SPY-C here stands for **S**paFHy-**P**hydro-**Y**asso for **C**arbon calculation.

2.1.1 Plant hydraulic and photosynthesis module (Phydro)

Phydro is based on Joshi et al. (2022), which unifies plant photosynthesis and hydraulics through a trait-based optimality theory implemented through a single cost-benefit function. The first principle in Phydro is the steady-state leaf water balance, that is, the hydraulic flow rate at which water enters the leaf (the left side of Eq. 1) equals the transpiration rate (the right side of Eq. 1):

$$-\frac{K_p}{\eta}\int_{\psi_s}^{\psi_s-\Delta\psi} P(\psi)\,d\psi = 1.6 g_s D. \tag{1}$$

Here, K_p (m) is the maximum whole-plant conductance per unit leaf area. η (Pa s) is the dynamic viscosity of water, which is a function of air temperature ($\mathbf{T}$) and pressure ($\mathbf{P_{atm}}$). Note that we denote all the model input variables by bold. ψ_s (Pa) is

https://doi.org/10.5194/egusphere-2025-5972
Preprint. Discussion started: 12 December 2025

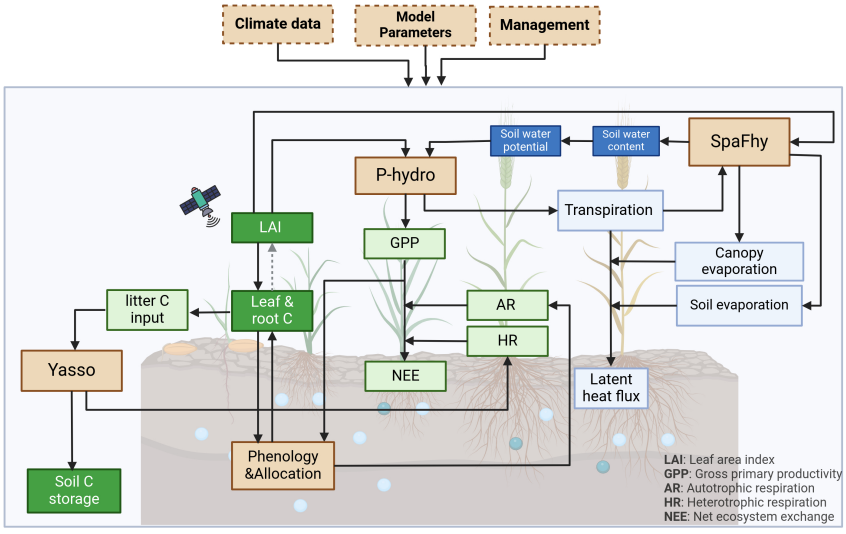

Figure 1. The model structure of SPY-C. Beige boxes denote the major model components and input data. The light and dark green boxes denote carbon fluxes and storages. The light and dark blue boxes denote water fluxes and storages.

the soil water potential. $\Delta\psi$ (Pa) is the difference in water potential between the soil and the leaf. g_s (mol/m^2/s) is the stomatal conductance to CO_2. D is the vapor pressure deficit (**VPD**) divided by $\mathbf{P_{atm}}$. $P(\psi)$ is the vulnerability curve (Eq. 2) that describes the decline in plant water conductance $K(\psi)$ with its water potential (ψ) (Eq. 3):

$$P(\psi) = (1/2)^{(\psi/\psi_{50})^b}, \tag{2}$$

$$K(\psi) = K_p P(\psi), \tag{3}$$

where ψ_{50} is the water potential at which 50% of hydraulic conductivity is lost, and b determines the sensitivity of conductivity loss to water potential.

The second principle is the photosynthetic coordination hypothesis, which states that under typical day time conditions the photosynthetic capacity is optimized so that the carboxylation-limited photosynthesis rate A_c (i.e., the left side of Eq. 4) and light-limited photosynthesis rate A_j (i.e., the right side of Eq. 4) are equal:

$$V_{cmax}\frac{c_i - \Gamma^*}{c_i + K_M} - R_d = \frac{J}{4}\left(\frac{c_i - \Gamma^*}{c_i + 2\Gamma^*}\right) - R_d. \tag{4}$$

Here, V_{cmax} ($umol\ m^{-2}s^{-1}$) is the maximum carboxylation capacity of leaves. c_i is the leaf-internal CO_2 partial pressure divided by $\mathbf{P_{atm}}$. K_M and Γ^* are the Michaelis-Menten coefficient for C_3 photosynthesis, and the photosynthetic light-compensation point, respectively. Both are a function of $\mathbf{T}$ and $\mathbf{P_{atm}}$. R_d is the dark respiration, which is assumed to be

https://doi.org/10.5194/egusphere-2025-5972
Preprint. Discussion started: 12 December 2025

proportional to V_{cmax} (Eq. 5). J ($umol\ m^{-2}s^{-1}$) is the effective electron transport capacity of leaves, which is described by Eq. 6. We note that there are still uncertainties on the time scale on which the optimisation of photosynthetic capacity operates, spanning from instantaneous to weekly time scales (Joshi et al., 2022). Here, we assume that the optimization occurs at an hourly time scale to be tightly coupled with soil moisture dynamics during the day.

$$R_d = b_r V_{cmax}, \tag{5}$$

where b_r is a unitless coefficient set to 0.015 in this study (Atkin et al., 2015).

$$J = \frac{4\phi_0 I_{abs}}{\sqrt{\left(\frac{4\phi_0 I_{abs}}{J_{max}}\right)^2 + 1}}, \tag{6}$$

where ϕ_0 is the intrinsic quantum-yield efficiency, which is a function of $\mathbf{T}$, J_{max} ($\mu mol\ m^{-2}s^{-1}$) is the maximum electron transport capacity of leaves under light saturation, I_{abs} ($\mu mol\ s^{-1}m^{-2}_{leaf}$) is the incident photosynthetic photon-flux density per unit leaf area, which is calculated following Eq. 7.

$$I_{abs} = \mathbf{PAR} f_{apar} / \mathbf{LAI}, \tag{7}$$

where $\mathbf{PAR}$ is photosynthetically active radiation ($\mu mol\ m^{-2}s^{-1}$), $\mathbf{LAI}$ (m^2m^{-2}) is the total one-sided green leaf area per unit ground surface area, and f_{apar} is the fraction of absorbed photosynthetically active radiation by the plant, which can be approximated following Beer's law:

$$f_{apar} = 1 - e^{-k\mathbf{LAI}}, \tag{8}$$

where k is the canopy light attenuation parameter, which is assumed to be 0.5 in this study.

The third principle is the steady-state leaf CO_2 balance, which states that the rate of photosynthesis (the left side of Eq. 9, based on Eq. 4), equals the rate at which CO_2 diffuses into the leaves (the right side of Eq. 9):

$$\frac{J}{4} \cdot \frac{c_i(1-b_r) - (\Gamma^* + b_r K_M)}{c_i + 2\Gamma^*} = g_s \mathbf{c_a}(1-\chi). \tag{9}$$

Here, $\mathbf{c_a}$ is the atmospheric CO_2 partial pressure divided by $\mathbf{P_{atm}}$ and χ is the ratio of c_i and $\mathbf{c_a}$.

Furthermore, a cost-benefit function F ($umol\ m^{-2}s^{-1}$) is defined for plants as the benefit of net photosynthetic assimilation (A_j) minus the costs of maintaining the photosynthetic capacity (J_{max}) and the hydraulic pathway ($\Delta\psi$), as given by Eq. 10:

$$F = A_j - \alpha J_{max} - \gamma \Delta\psi^2. \tag{10}$$

Here, α is a unitless coefficient denoting the unit cost of maintaining photosynthetic capacity, such as the regeneration of RuBP and electron transport proteins. γ ($umol\ m^{-2}s^{-1}Pa^{-2}$) denotes the unit cost of maintaining the plant hydraulic pathway, such as the construction cost to build xylem vessels and fibres. It is assumed that plants have adapted to their living environment in such a way that they can modulate their stomatal conductance g_s (and thus $\Delta\psi$ according to Eq. 1) and their electron-transport capacity J_{max} independently to maximise their net profit F.

https://doi.org/10.5194/egusphere-2025-5972
Preprint. Discussion started: 12 December 2025

Using Eqs.1-9, the variable A_j in Eq. 10 can be expressed as a function of J_{max} and $\Delta\psi$. As a result, finding the values of J_{max} and $\Delta\psi$ that maximize F becomes a two-dimensional bound-constrained optimisation problem and can be solved using a two-dimensional root finding algorithm (Morales and Nocedal, 2011).

With J_{max} and $\Delta\psi$ being determined, plant gross primary productivity (GPP, $umol\ m^{-2}s^{-1}$) and transpiration (Tr, $umol\ m^{-1}s^{-1}$) can be calculated according to Eq. 11 and 12:

$$GPP = (A_j + R_d) \cdot LAI, \tag{11}$$

$$Tr = 1.6 g_s D \cdot LAI, \tag{12}$$

where factor 1.6 accounts for the relative diffusivity of water vapor to that of CO_2, and A_j, R_d, and g_s are from Eq. 4, 5, and 1, respectively.

2.1.2 Soil water balance module SpaFHy

The soil water balance in SPY-C describes the processes such as infiltration, drainage, and evapotranspiration (ET), the latter consisting of plant transpiration (Eq. 12) and soil evaporation. We adopted representations of rainfall interception, snow accumulation and melt, and a single-layer soil water balance from the SpaFHy (Spatial Forest Hydrology, Launiainen et al., 2019) model. The hydrological processes can be simulated at hourly resolution to enable close coupling with Phydro. The simulated volumetric soil water content is converted to soil water potential using the van Genuchten soil water retention function (Schaap and Van Genuchten, 2006) and passed to Phydro as an input variable (Fig. 1 and Eq. 13):

$$\psi_s = -\frac{1}{\alpha_v}(S_e^{-\frac{1}{m}} - 1)^{\frac{1}{n}}, \tag{13}$$

where ψ_s (kPa) is the soil water matric potential and α_v, n, and m are empirical shape parameters. The parameter m is commonly expressed as $m = 1 - \frac{1}{n}$. S_e is the effective saturation as given by Eq. 14:

$$S_e = \frac{\theta - \theta_r}{\theta_s - \theta_r}, \tag{14}$$

where θ is the volumetric soil water content (m^3/m^{-3}), θ_s is the saturated soil water content, and θ_r is the residual water content.

To be consistent, the soil hydraulic conductivity (K_{soil}) affecting drainage and soil to root water transport is also derived using the van Genuchten model (Schaap and Van Genuchten, 2006), which can be written as:

$$K_{soil} = K_{sat} S_e^{0.5}(1 - (1 - S_e^{1/m})^m)^2. \tag{15}$$

Here, K_{sat} ($m\ s^{-1}$) is the saturated hydraulic conductivity. Total ET is the sum of canopy, soil evaporation, and transpiration flux simulated by Phydro (Fig. 1).

https://doi.org/10.5194/egusphere-2025-5972
Preprint. Discussion started: 12 December 2025

2.1.3 Phenology and allocation module

The phenology and carbon allocation module (PA) directly allocates daily assimilated carbon ($\overline{GPP}$) into above- (i.e., leaf) and below-ground (i.e., root) carbon pools according to specific allometric ratios, following the concept from Sierra et al. (2022) (Eq. 16 and 17).

$$CF_{gpp:leaf} = \overline{GPP} \cdot a_{leaf}, \tag{16}$$

$$CF_{gpp:root} = \overline{GPP} \cdot a_{root}, \tag{17}$$

where $\overline{GPP}$ denotes the daily accumulation of hourly GPP flux derived by Eq. 11, $CF_{gpp:leaf}$ and $CF_{gpp:root}$ ($umol\ m^{-2}d^{-1}$) are the carbon fluxes from $\overline{GPP}$ to leaf and root, and a_{leaf} and a_{root} are the respective proportions of $\overline{GPP}$ allocated to leaf and root carbon storage at each daily time step. For cereal crops, grains can constitute a significant proportion of the aboveground biomass. The grain filling flux ($CF_{gpp:grain}$) is thus considered and described following Eq. 18:

$$CF_{gpp:grain} = \overline{GPP} \cdot a_{grain}, \tag{18}$$

where a_{grain} denotes the proportion of $\overline{GPP}$ allocated to grain carbon pool at each daily time step. The details on how a_{leaf}, a_{root}, and a_{grain} are derived and constrained by observation can be found in Methods S1 in the Supporting Information (SI).

The newly allocated carbon is then subject to autotrophic respiration (AR), consisting of growth ($CF_{gr,leaf}$, $CF_{gr,root}$, $CF_{gr,grain}$) and maintenance respiration ($CF_{mr,leaf}$, $CF_{mr,root}$, $CF_{mr,grain}$) of the plant organs. In addition, it is assumed that both leaf and root lose their carbon through turnover ($CF_{leaf:litter}$, $CF_{root:litter}$), which produces litter carbon input to soil (Fig. 1). More detailed formulation of these fluxes can also be found in Methods S1.

The changes in carbon storage of leaf (ΔCS_{leaf}), root (ΔCS_{root}), and grain (ΔCS_{grain}) at each time step are given by Eq. 19–20–21, respectively:

$$\Delta CS_{leaf} = CF_{gpp:leaf} - CF_{leaf:litter} - CF_{mr,leaf} - CF_{gr,leaf}, \tag{19}$$

$$\Delta CS_{root} = CF_{gpp:root} - CF_{root:litter} - CF_{mr,root} - CF_{gr,root}, \tag{20}$$

$$\Delta CS_{grain} = CF_{gpp:grain} - CF_{mr,grain} - CF_{gr,grain}. \tag{21}$$

2.1.4 Soil decomposition module YASSO

We describe soil carbon balance dynamics and heterotrophic respiration (HR) using a daily timestep version of YASSO20 soil carbon model (Viskari et al., 2022; Heimsch et al., 2024). The litter input ($CF_{leaf:litter}$, $CF_{root:litter}$) is provided by the PA

https://doi.org/10.5194/egusphere-2025-5972
Preprint. Discussion started: 12 December 2025

module (Eq. S8 and S9) and the litter quality (i.e., carbon fractions) is prescribed depending on crop types following the study by Palosuo et al. (2015).

Combining the HR derived from YASSO with the autotrophic respiration flux (AR) calculated in the PA module (Eq. S7) sum up to the total ecosystem respiration ($RECO$):

$$RECO = AR + HR. \tag{22}$$

Further, combining $\overline{GPP}$, the net ecosystem exchange (NEE) at a daily time step (Fig. 1) can be expressed as:

$$NEE = RECO - \overline{GPP}. \tag{23}$$

2.2 Model experiments

2.2.1 Study sites and observation data

Two mineral soil crop fields from Southern Finland were used in this study (Fig. 2a). The Qvidja site (60.29550 °N, 22.39281°E; elevation 5 m) is on the southwestern coast of Finland, which has continuous eddy covariance (EC) flux measurements since May 2018 (Heimsch et al., 2021). The footprint area of the flux measurement was covered by a mixture of perennial grasses and legume dominated by timothy (*Phleum pratense*), meadow fescue (*Festuca pratensis*), and white clover (*Trifolium repens*) during the study period. The soil is a relatively fine textured clay loam. The Hauho site (61.13977 °N, 24.58401°E; elevation 89.5 m) has continuous EC measurements since June 2022 (Vira et al., 2025). The footprint area of the flux measurement is mainly covered by oat (*Avena sativa*) and in 2023, Italian ryegrass (*Lolium multiforum*) was also sown as a cover crop during the growing season. Unlike Qvidja, Hauho has a coarser soil texture (silty loam). The difference between the two sites in crop types, soil properties, and management offers a good test of the capabilities of the model. For the simplicity and clarity of our following text, we refer to the Qvidja and Hauho sites as the GRASS and OAT sites, respectively.

The EC instrumentation at both sites was the same, measuring CO_2/H_2O mixing ratio (LI-7200, LI-COR Biosciences, USA), and three-dimensional wind at 10 Hz frequency (u-Sonic3 Scientific, METEK GmbH, Germany). Besides flux measurements, auxiliary meteorological measurements close to the EC tower were also performed, such as air temperature and relative humidity (Humicap HMP155, Vaisala Oyj, Finland), photosynthetically active radiation, soil temperature (-5 or -10 cm; Pt100 IKES sensors, Nokeval Oy, Finland), and soil moisture (-5 or -10 cm; ML3 ThetaProbe sensor, Delta-T Devices Ltd., UK). The half-hourly turbulent CO_2/H_2O fluxes were calculated using the Eddypro software (v. 7.0.9, LI-COR Biosciences, USA), following standard quality control and filtering protocols (Vira et al., 2025). The gap-filling of the flux data was performed using the method developed by Vekuri et al. (2023). As environmental drivers in the gap-filling, we used air and soil temperature, photosynthetically active radiation, soil moisture, and VPD for both sites, and for the GRASS site also LAI and precipitation. NEE was partitioned into GPP and RECO. RECO was assumed to follow an Arrhenius-type temperature response function (Lloyd and Taylor, 1994) and parameters were fitted following Reichstein et al. (2005). Parametrization of GPP was based on a nonlinear radiation response function as in Gerin et al. (2023). Both sites experienced meteorological droughts of various severity during the observation periods, which was manifested in both soil and atmosphere (Fig. 2e,f). For

https://doi.org/10.5194/egusphere-2025-5972
Preprint. Discussion started: 12 December 2025

more detailed information about the sites and data, we refer to the aforementioned references, as well as the Field Observatory (https://fieldobservatory.org), which is an open platform for real-time monitoring of crop fields in Finland (Nevalainen et al., 2022a).

2.2.2 Model initialization

All input data required to parameterize and run SPY-C are summarised in Methods S2. The simulations for the GRASS and OAT sites with SPY-C were set to start on 01.01.2018 and 01.01.2022, respectively, and end on 31.12.2023. The meteorological forcing data for the two sites were obtained from global ERA5-Land reanalysis data (Muñoz-Sabater et al., 2021). The annual LAI cycle was prescribed by interpolating the LAI extracted from Sentinel-2 remote sensing products to daily values (Fig. 2c) using a Gaussian process regression as described in Vira et al. (2025). The retrieval of LAI was based on Sentinel-2 level-2A (bottom-of-atmosphere reflectance) products and follows the LAI algorithm (v1.1) developed by Weiss et al. (2020) for the European Space Agency's SNAP software (Science Toolbox Exploitation Platform) and implemented in the satellitetools Python package (https://doi.org/10.5281/zenodo.5993291).

As the model simulations started in winter, soil moisture was initialized with a full saturation state, which is consistent with soil moisture measurements at the study sites (Fig. 2e,f). The soil depth for root water uptake is set to 0.6 m, which was found to well represent the storage of the root zone available water (Methods S3) and reproduce the observed dynamic of surface soil moisture at both study sites (Fig. S1). The parameters for the soil water retention function (Eq. 13) were selected by comparing the volumetric soil moisture range measured at both study sites with the soil water retention curves (SWRC) established for the major types of Finnish forest soils by Launiainen et al. (2022) (Fig.2b). These SWRCs are considered representative for Finnish soils in general. It is shown that SWRC5 and SWRC4 best encompass the range of measured soil moisture in the GRASS and OAT sites, respectively. They were therefore chosen for the simulations of each site. The lower wilting point of SWRC4 for the OAT site than that of SWRC5 for the GRASS site is consistent with the coarser soil texture observed in the OAT site. We also selected SWRC3 for the simulations at the GRASS sites. Compared to SWRC5, SWRC3 can give rise to a lower soil water potential (i.e., higher soil water stress) under the same volumetric soil moisture (Fig. 2b). This allows us to better illustrate the impact of soil water stress at the study site.

The initialization of the soil organic carbon pools in SPY-C was performed by firstly assuming the relative fractions of the four faster-cycling carbon pools in YASSO are in a steady state with a fixed litter carbon composition according to the study by Palosuo et al. (2015) and mean climatology. Meanwhile, the slowest-cycling carbon pool (humus) was set to hold a prescribed carbon fraction (referred to as legacy carbon) that does not equilibrate with the input carbon. Secondly, the relative fractions of different soil carbon pools were rescaled to match the observed total soil organic carbon stock in the 0-100 cm soil layer, which was set to 16.0 (measured range: 14.3–18.8) kg m^{-2} for the GRASS site (Heimsch et al., 2021), and 12.0 (measured range: 8.5–15) kg m^{-2} for the OAT site (Fig. S2). We tuned the legacy carbon fraction to match the observed $RECO$ flux in both the GRASS and the OAT sites, and the values were 0.3 and 0.1 for the GRASS and OAT sites, respectively. The lower fraction of the legacy carbon (i.e., the most recalcitrant carbon pool) for the OAT site is in line with its coarser soil texture and thus less mineral-protected stable carbon (Haddix et al., 2020).

https://doi.org/10.5194/egusphere-2025-5972
Preprint. Discussion started: 12 December 2025

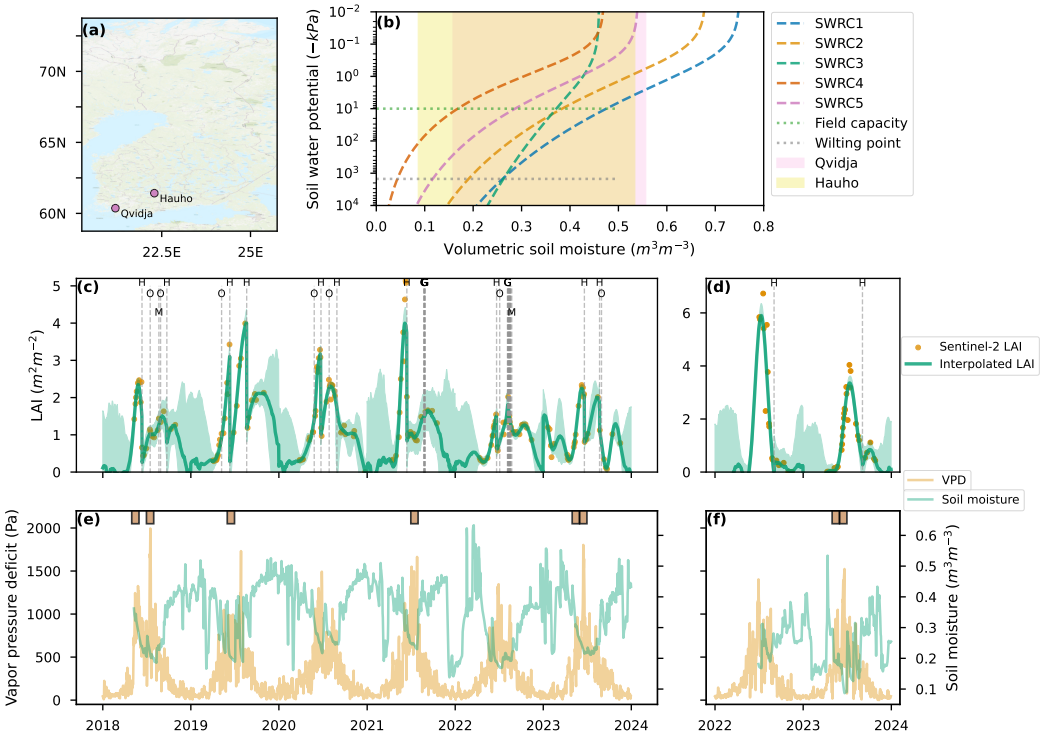

Figure 2. The location of the study sites (a), the five representative soil water retention curves (dashed lines) found for Finnish forest soils (Launiainen et al., 2022) together with the measured range of volumetric soil moisture (coloured areas) at the study sites (b), the observed leaf area index (LAI) from Sentinel-2 (dots) and daily LAI (line) interpolated for Qvidja (the GRASS site) (c) and Hauho (the OAT site) (d), and the daily vapor pressure deficit and soil moisture observed at the GRASS and OAT sites are shown in (e) and (f). The management events included in the simulations are shown in (c) and (d). H: Harvest; O: Organic fertilizer; G: Grazing. The meteorological drought months according to the Standardised Precipitation-Evapotranspiration Index (SPEI) (<-1.5) from global SPEI database (https://spei.csic.es/database.html) are denoted by brown bars in (e) and (f).

2.2.3 Parameter perturbation ensemble and sensitivity analysis

To deduce hydraulic traits of the crops and their impacts on productivity and drought resistance, we selected four tunable Phydro parameters for parameter perturbation ensemble (PPE) experiments (see Table 1). Three of them (i.e., K_p, ψ_{50} and γ) are relevant to plant hydraulics while one (i.e. α) is related to plant photosynthetic activity. In each PPE, four evenly spaced values were drawn from the prior range of each parameter and randomly combined with each other to form a member of the PPE (Table 1). In total, 256 members were included.

The prior ranges of each parameter were defined based on the existing literature. For hypothetical parameters such as α and γ in Phydro, the ranges were directly from Joshi et al. (2022), who examined various plant species. For the measurable hydraulic traits, i.e., K_p and ψ_{50}, the ranges from Joshi et al. (2022) are shown to be $[0.2, 15.9]e^{-16}$ m, and $[-2.2, -0.4]$ MPa,

https://doi.org/10.5194/egusphere-2025-5972
Preprint. Discussion started: 12 December 2025

respectively. However, due to the limited number of herbaceous species studied in Joshi et al. (2022), we refined the prior ranges using existing observational studies on herbaceous crops (Table S3). K_p was set to [0.5, 10]e^{-16} m and ψ_{50} to $[-3, -1]$ MPa, which align with the values reported in previous crop studies (Table S3) and likely cover those of boreal crops as well.

Table 1. Summary of the prior range of the Phydro parameters for parameter perturbation ensemble (PPE) experiments. The 5 best-fit Phydro parameter sets for perennial grass, oat and cover crop mixture are also listed. K_p: the maximum whole-plant conductance per unit leaf area ($10^{-16}m$). ψ_{50}: the water potential at which plant lose its 50% of hydraulic conductivity (MPa). α: the unit cost of maintaining photosynthetic capacity. γ: the unit cost of maintaining plant hydraulic pathways. cor_{gpp} and cor_{et}: the correlation coefficients between model and observation for GPP and ET, respectively. $nmse_{gpp}$ and $nmse_{et}$: the normalized mean squre error between model and observation for GPP and ET, respectively.

Parameters	K_p	Φ_{50}	α	γ	cor_{gpp}	$nmse_{gpp}$	cor_{et}	$nmse_{et}$
Prior range	$[0.5, 10]$	$[-3, -1]$	$[0.03, 0.12]$	$[0.1, 5]$				
Five best-fit PPE members								
Perennial grass	0.5	-1	0.06	3.36	0.940	0.067	0.938	0.158
	0.5	-1.7	0.06	3.36	0.941	0.066	0.939	0.165
	0.5	-1.7	0.03	5.00	0.939	0.081	0.939	0.165
	0.5	-2.3	0.06	5.00	0.941	0.068	0.934	0.142
	0.5	-3.0	0.06	5.00	0.941	0.067	0.935	0.142
Oat	0.5	-1.0	0.03	3.36	0.963	0.059	0.905	0.115
	0.5	-1.7	0.03	3.36	0.964	0.056	0.906	0.115
	0.5	-1.7	0.06	1.73	0.965	0.087	0.908	0.123
	0.5	-2.3	0.03	3.36	0.965	0.055	0.907	0.115
	0.5	-3.0	0.03	5.00	0.964	0.059	0.902	0.115
Cover crop mixture	3.7	-1.7	0.03	3.36	0.817	0.201	0.785	1.700
	3.7	-3.0	0.06	1.73	0.818	0.245	0.786	1.995
	3.7	-1.0	0.06	1.73	0.812	0.257	0.786	2.065
	6.8	-1.7	0.06	5.00	0.816	0.247	0.787	2.195
	6.8	-1.0	0.06	5.00	0.830	0.250	0.787	2.232

The main PPE experiments performed in this study are summarised in Table 2. For the GRASS site, two PPE experiments were performed: One using SWRC5 (QV_ctrl) and one using SWRC3 (QV_swrc3). To further separate the impact of soil drought from that of atmospheric drought, two additional sets of PPE experiments were performed: One using fully saturated soil moisture (QV_fullSM) and one using very low VPD (<=50 Pa) (QV_noVPD) for the whole simulation periods. The impact of soil (atmospheric) drought can then be deduced by comparing the difference between QV_fullSM (QV_noVPD) and QV_ctrl. The PPE experiments performed for the OAT site (HA_ctrl, HA_fullSM, HA_noVPD) were the same as those for the GRASS site, except that SWRC4 was used in all its PPEs (Table 2).

https://doi.org/10.5194/egusphere-2025-5972
Preprint. Discussion started: 12 December 2025

Table 2. Summary of the settings of the major parameter perturbation ensemble (PPE) experiments performed and analyzed in this study.

Experiments ID	Sites	Crop type	Phydro Parameters	SWRC	Soil moisture	VPD
QV_ctrl	Qvidja	Perennial forage grass	PPE(256)	SWRC5	Prognostic	Observed
QV_swrc3	Qvidja	Perennial forage grass	PPE(256)	SWRC3	Prognostic	Observed
HA_ctrl	Hauho	Oat	PPE(256)	SWRC4	Prognostic	Observed
QV_fullSM	Qvidja	Perennial forage grass	PPE(256)	SWRC5	Saturated	Observed
HA_fullSM	Hauho	Oat	PPE(256)	SWRC4	Saturated	Observed
QV_noVPD	Qvidja	Perennial forage grass	PPE(256)	SWRC5	Prognostic	<=50 Pa
HA_noVPD	Hauho	Oat	PPE(256)	SWRC4	Prognostic	<=50 Pa

The PPE experiments QV_ctrl and HA_ctrl were used to select the PPE members that best reproduced the observed daily GPP and ET fluxes at the study sites. The apparent hydraulic traits for the crop at each study site can thus be inversely retrieved. Due to the close coupling between plant photosynthesis and hydraulics, we anticipated that employing both GPP and ET fluxes would impose tighter constraints on the four perturbed Phydro parameters compared to using only one flux. To achieve this, we calculated the Pearson correlation coefficient (cor) and normalized mean square error ($NMSE$) defined in Eq. 24 and Eq. 25 for each PPE member. The PPE members (five in total) that ranked highest in cor and lowest in $NMSE$ for both GPP and ET were selected, and the corresponding Phydro parameters were regarded as the "best-fit" parameters for the simulated crops. More details on the ranking algorithm can be found in Methods S4. We note that both cor and $NMSE$ were calculated using daily data here to emphasise the model's ability in reproducing daily variabilities and subseasonal drought responses. Calculations using monthly data yielded similar results and thus are not shown here.

$$cor = \frac{\sum_{i=1}^{n}(X_{obs,i} - \mu_{obs})(X_{sim,i} - \mu_{sim})}{\sqrt{\sum_{i=1}^{n}(X_{obs,i} - \mu_{obs})^2 \sum_{i=1}^{n}(X_{sim,i} - \mu_{sim})^2}} \tag{24}$$

$$NMSE = \frac{\sum_{i=1}^{n}(X_{obs,i} - X_{sim,i})^2}{\sum_{i=1}^{n} X_{obs,i}^2}, \tag{25}$$

https://doi.org/10.5194/egusphere-2025-5972
Preprint. Discussion started: 12 December 2025

where i is the time step and n is the total number of time steps, $X_{obs,i}$ and $X_{sim,i}$ are the observed and simulated values at each time step, μ_{obs} and μ_{sim} are the respective mean values over all time steps. Here, the time periods chosen for the calculation of these matrices (i,e., benchmarking periods) were 01.2019–12.2022 and 06.2022–12.2023 for the GRASS and OAT sites, respectively. Due to sowing events in 2018 and 2023 at the GRASS site, we excluded those years from the site's benchmark period. Instead, we employed them as additional tests to assess the transferability of the selected best-fit parameters beyond the benchmark periods. More detailed exploration on utilising different benchmarking periods can be found in Methods S4.

To better gauge the effects of crop hydraulic traits on crop performance and drought response, the Morris sensitivity analysis (Morris, 1991) was also conducted using the PPE experiments for both sites. The sensitivities of monthly GPP, ET, and water use efficiency (WUE) to the 4 Phydro parameters perturbed in PPE were quantified. Here, WUE was measured at both the plant level ($pWUE$) as given by:

$$pWUE = GPP/Tr, \tag{26}$$

and the leaf level, often called intrinsic WUE ($iWUE$) as given by:

$$iWUE = (A_j + R_d)/1.6g_s. \tag{27}$$

The Morris method is an efficient global sensitivity analysis technique for parameter screening (Campolongo et al., 2007), especially with a limited sampling size (Gan et al., 2014). It is similar to the commonly used one-at-a-time sensitivity analysis, yet also considers the interactions among parameters. The overall effect and interaction effect of each parameter are approximated by the mean (mu) and standard deviation ($sigma$) of the elementary effects of each parameter sampled. In addition, the mean of absolute effects (mu^*) is also used to indicate if the elementary effects are of opposite signs (Campolongo et al., 2007). The analysis was performed using the Python package SALIB, version 1.4.8 (Herman and Usher, 2017).

3 Results

3.1 Crop hydraulic traits and performance at GRASS and OAT sites

We identified the Phydro parameter sets that reproduced daily GPP and ET with high accuracy at both sites (Table 1 and Fig. 3). As shown in Fig. 3a-d, the best-fit Phydro parameter sets resided in the region of low K_p but higher γ, indicating a conservative water-use strategy with relatively low hydraulic efficiency for both perennial grass and oat. A low α (i.e., cost to maintain photosynthetic capacity) was also required to reproduce the observed fluxes at both sites, implying high photosynthetic capacity in both crops (Fig. S3). Compared to perennial forage grass, the best-fit parameter sets for oat showed slightly lower α and γ (Table 1 and Fig. 3a–d), pointing to a higher photosynthetic capacity and a more acquisitive hydraulic strategy in oat. The cover crop mixture (the blue plus in Fig. 3a, b) exhibited higher K_p, suggesting greater hydraulic efficiency than either oat or perennial grass. There was no discernible preference for ψ_{50} (the trait commonly used to reflect hydraulic safety) across the best-fit parameter sets for the studied crops, in contrast to the other 3 Phydro parameters.

https://doi.org/10.5194/egusphere-2025-5972
Preprint. Discussion started: 12 December 2025

Fig. 3e–l show how the five best-fit PPE members selected for perennial grass and oat perform in simulating daily GPP and ET. Overall, the simulated GPP and ET matched the observed fluxes very well, with $cor \approx 0.94$ and $NMSE \leq 0.14$ for the GRASS site, and $cor \geq 0.91$, $NMSE \leq 0.11$ for the OAT site. Only a slight overestimation of daily ET was observed at the GRASS site (Fig. 3h), and a mismatch of ET occurred at the OAT site in the early spring 2023 when the model failed to capture the observed high ET (Fig. 3k), largely due to the bias in the onset of snowmelt in the meteorological forcing data (Fig. S7). The observed dirunal cyles of GPP and ET in summer were also well captured by the best-fit PPE members (Fig. 4). There was a slight underestimation (overestimation) of GPP (ET) in early morning and late afternoon, probably resulting from a different light absorption rate from what was assumed in the model (see Eq. 8) due to the low sun angle.

We further examined crop performance in the context of the full PPE experiments spanning a wide hydraulic and photosynthetic trait space (Fig. 5). For GPP, the best-fit PPE members generally fell in the upper range of the full PPE (Fig. 5a, b), except in May at the GRASS site when they shifted towards the lower end of the spread. But for ET, the best-fit PPE members tended to lie in the lower range (Fig. 5c, d), except during dry summer months at the GRASS site (June 2018, 2019, 2023; July 2021) and the OAT site (July–August 2022). Consequently, their monthly mean pWUE and iWUE were close to the upper limit of the PPE, except in those same drought periods (Fig. 5e–h). Notably, the soil moisture simulated in the best-fit PPE members consistently lies in the upper range of the PPE (Fig. 5i–j), far above the wilting point.

3.2 Sensitivity of crop performance to hydraulic traits

The Morris sensitivity analysis of GPP, ET, pWUE, and iWUE to the four Phydro parameters is shown in Fig. 6a–h. The sensitivities are context-dependent and vary seasonally, but do not differ much between the two crop types examined here. GPP is dominated by negative sensitivity to α (the cost to maintain photosynthetic capacity) throughout the growing season, except in June–July, when K_p and γ exert strong negative and positive effects, respectively, suggesting that lower hydraulic efficiency can promote crop productivity during these months. ET, pWUE, and iWUE exhibit more pronounced sensitivity to the hydraulic parameters (i.e., K_p and γ). In particular, K_p (γ) can negatively (positively) influence pWUE and iWUE in May, September, and October, while the effects often reverse in summer, highlighting a positive impact of hydraulic efficiency on pWUE and iWUE at peak growth, which is opposite to its impact on GPP.

We note that while the effects of α are quite independent of the other parameters (low $Sigma$), the effects of K_p and γ are more dependent on the other parameters (high $Sigma$), indicating strong coordination among crop hydraulic traits. We observe little influence of ψ_{50} on GPP, ET, and WUE at both study sites, but a noticeable positive effect on soil moisture in summer (Fig. 6i, j). A uniform negative (positive) effect of K_p (γ) on soil moisture (Fig. 6i, j) suggests that lower crop hydraulic efficiency can better conserve soil water from being drained by the crop.

3.3 Response to soil and atmospheric drought

As illustrated in Fig. 7, the absence of soil drought and VPD increases GPP during the summer months in most PPE members (Figs. 7a–d) with the magnitude of the increase positively related to K_p. In contrast, transpiration responds differently to the absence of soil versus atmospheric droughts (Fig. 7e–h): removing soil drought produces a consistently positive change, whereas

https://doi.org/10.5194/egusphere-2025-5972
Preprint. Discussion started: 12 December 2025

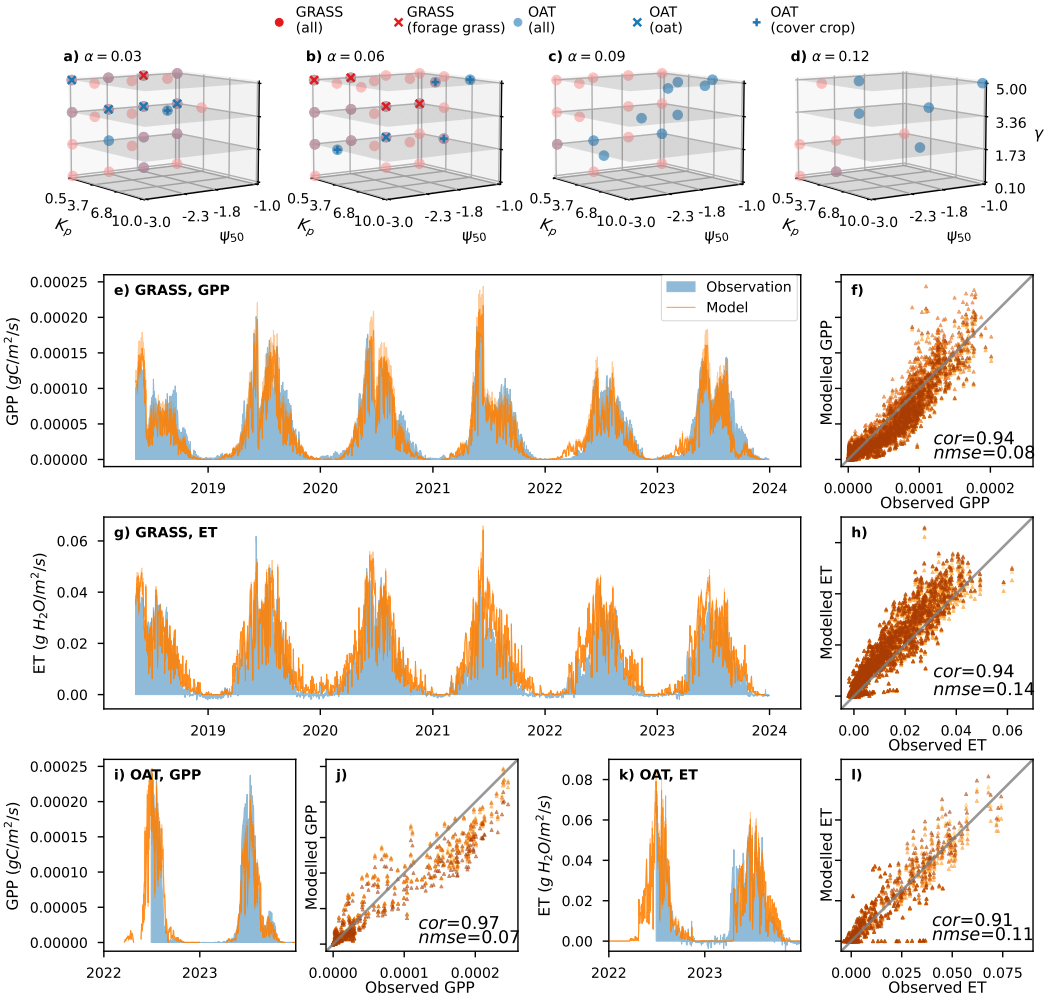

Figure 3. (a-d) The best-fit parameter sets selected for the GRASS (QV_ctrl) and OAT (HA_ctrl) site based on different benchmarking time periods (Methods S4). The positions of the five best-fit parameter sets selected using 01.2019-12.2022 and 06.2022-12.2023 as the benchmarking periods, representing forage grass and oat, are denoted by red and blue crosses, respectiely. The positions of the five best-fit parameter sets selected using 10.2023 as the benchmarking periods, representing cover crop mixture, are denoted by blue plus signs. (e-f) The simulated daily mean gross primary production (GPP), evapotranspiration (ET) and their comparison with the observation at the GRASS site. (i-l) same as (e-h), but for the OAT site. The results of QV_swrc3 can be found in Fig. S4.

reducing atmospheric drought induces a large spread with both positive and negative responses. Changes in transpiration are again most sensitive to K_p with positive effects mainly in summer.

The best-fit PPE members display little change in GPP and transpiration when soil drought is removed (Figs. 7a, b, e, f), indicating that crop photosynthesis and transpiration may have not suffered from soil drought, even though meteorological

https://doi.org/10.5194/egusphere-2025-5972
Preprint. Discussion started: 12 December 2025

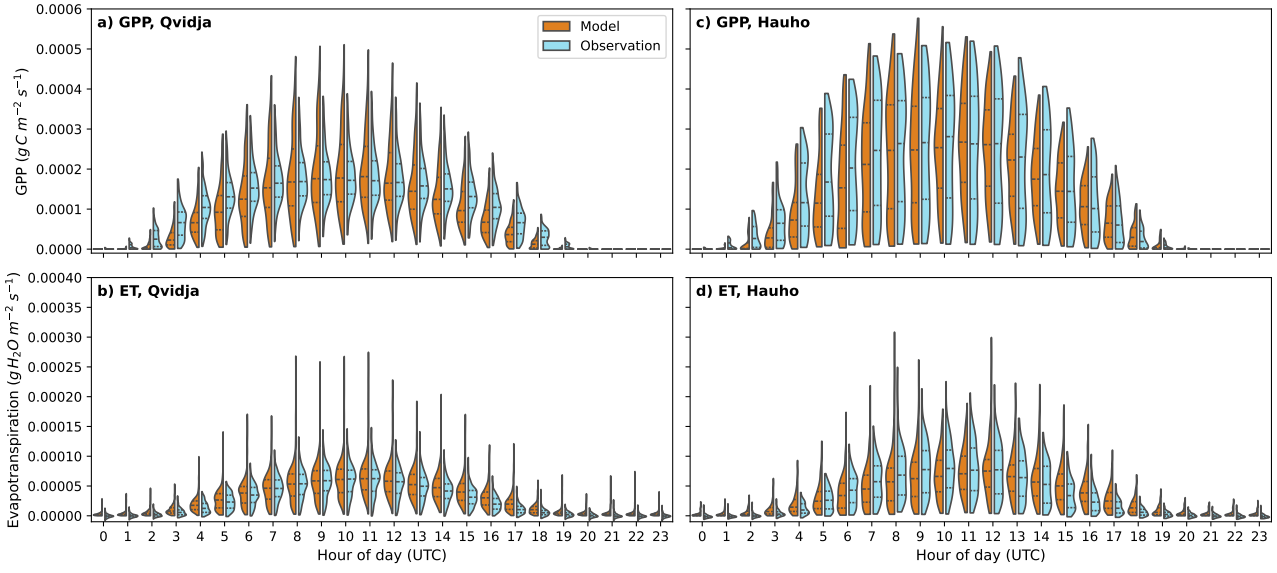

Figure 4. Daily cycle of GPP and ET fluxes in summer (June, July and August) from the best-fit PPE members and their comparison with observation at the GRASS site (a,b) and OAT site (c,d). For the GRASS and OAT site, the PPE QV_ctrl) and HA_ctrl were used, respectively.

droughts were widely observed at the study sites (Fig. 5i, j). In contrast, a discernible rise in GPP and a reduction in transpiration during summer is shown in the best-fit PPE members when removing atmospheric drought (Figs. 7c, d, g, h), suggesting that VPD may have exerted a more prevalent effect than soil drought at these sites.

The effect of VPD is further manifested in Fig. 8, where our simulations show a clear impact of VPD on the daily photosynthetic assimilation rate, pWUE, and iWUE (Fig. 8b, o, p) at both study sites. This can be explained by its strong regulation of stomatal conductance (Fig. 8d) and particularly soil-leaf water potential difference (Fig. 8l), which further impact leaf internal-to-external CO_2 ratio (χ) (Fig. 8h) and thus carboxylation and electron-transport capacity (Fig. 8f, j). The simulated effect of VPD appears to be quite non-linear. While the impact on hydraulic behaviours, such as stomatal conductance, pWUE, and iWUE, mainly occurrs in the early phase of VPD increase (VPD$\leq$0.8 kPa) (Fig. 8d, h, i, n, p), the downregulation of photosynthetic activity emerges only in the later phase (VPD$\geq$0.8 kPa) (Fig. 8b, f, j).

In comparison, soil drought and its impacts are hardly shown in the simulations of best-fit PPE members for the study sites, as soil water potential in these simulations remains well above the wilting point (Fig. 8a, c). The impacts of soil drought only emerge when using a more drought-prone SWRC (QV_swrc3), in which soil water potential declines below the wilting point during certain periods. There, photosynthetic capacity, assimilation rate, and stomatal conductance (Fig. 8a, c, e, i) decrease drastically, but pWUE and iWUE show an increase with lower soil water potential (Fig. 8m, o). Such response contrasts with the effect of increasing VPD, which tends to promote iWUE but reduce pWUE (cf. Fig. 8m, o and n, p).

https://doi.org/10.5194/egusphere-2025-5972
Preprint. Discussion started: 12 December 2025

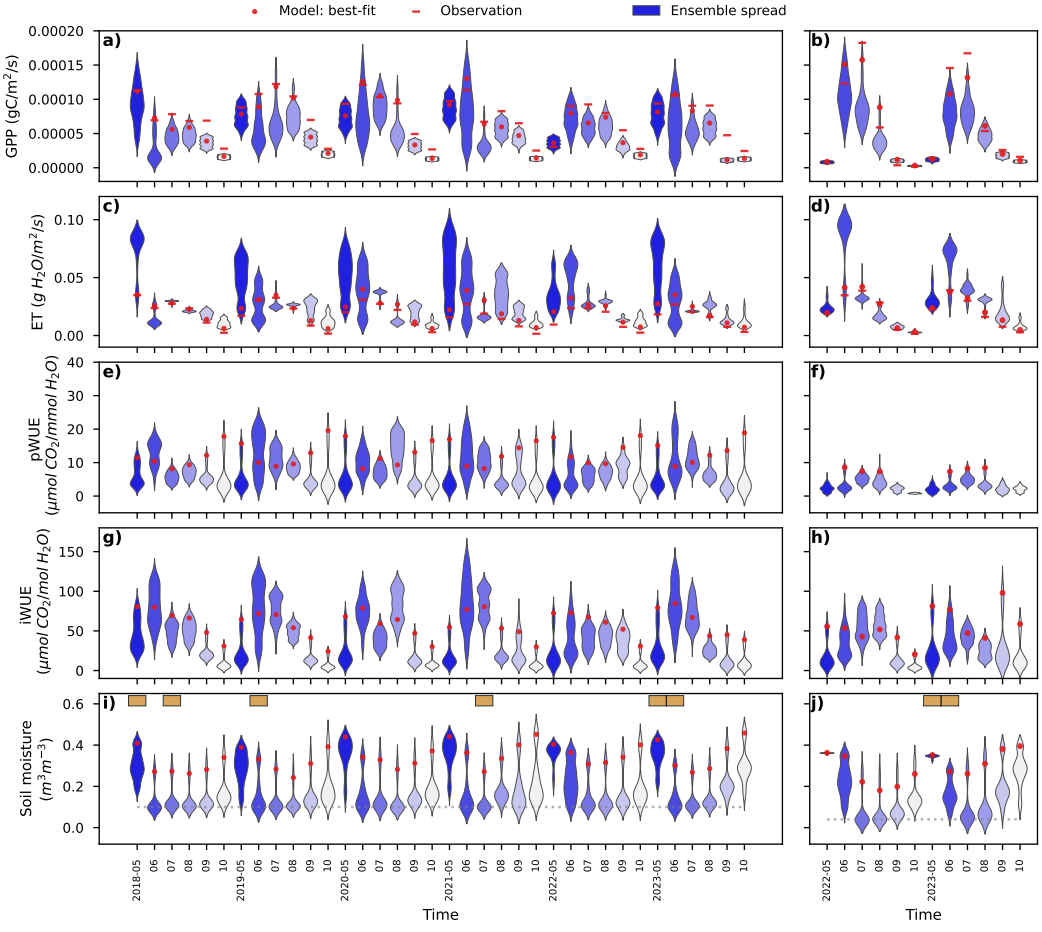

Figure 5. The violin plots showing the spread of monthly mean gross primary production (GPP), evapotranspiration (ET), water use efficiency (pWUE and iWUE), and soil moisture in the PPE of the GRASS (QV_ctrl) (a, c, e, g, i) and OAT sites (HA_ctrl) (b, d, f, h, j). The width of the violin denotes the probability density of the ensemble members that yield the same values. The red circles represent the mean of the five best-fit PPE members. The red bars denote the observation. The brown boxes in (i) and (j) denote meteorological drought months according to Standardised Precipitation-Evapotranspiration Index (SPEI) less than -1.5. The dotted line in (i) and (j) denote the wilting point. The results of QV_swrc3 can be found in Fig. S5.

4 Discussion

4.1 Hydraulic traits and coordination in boreal crops

By employing a unified model of plant hydraulic and photosynthesis (Phydro), we were able to gain insights into crop hydraulic traits and their impacts on crop performance in the boreal region, which has been overlooked in most of the boreal crop studies so far (Roitsch et al., 2022). Constrained by the observed carbon and water fluxes, the maximum hydraulic conductance of the

https://doi.org/10.5194/egusphere-2025-5972
Preprint. Discussion started: 12 December 2025

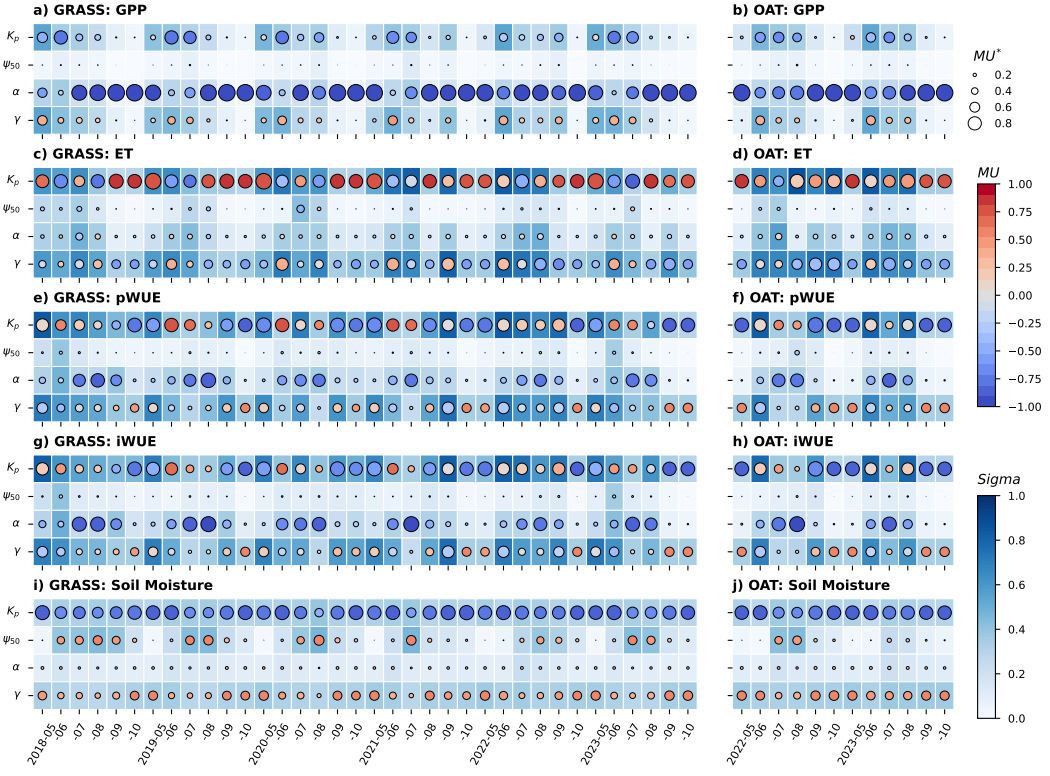

Figure 6. Morris' sensitivity analysis of monthly averaged gross primary production (GPP) (a, b), evapotranspiration (ET) (c, d), plant-level water use efficiency (pWUE) (e, f), internal water use efficiency (iWUE) (g, h) and soil moisture (i, j) to Phydro parameters (K_p, ψ_{50}, α, and γ) in the GRASS (QV_ctrl) and OAT (HA_ctrl) sites during growing season (May-October). The mean of the absolute elementary effect (MU^*) is denoted by the sized of the circle. The mean of the elementary effect (MU) is denoted by the colour shading of the circle. The standard deviation of the elementary effect ($Sigma$) is denoted by the colour shading of the rectangles. The results of QV_swrc3 can be found in Fig. S6 in the SI.

whole plant (K_p) was found to be in the lower range of the reported values for various crop species (cf., Table 1 and Table S3), suggesting an overall low hydraulic efficiency (i.e., conservative hydraulic strategy) of both annual (oat) and perennial (forage grass) varieties typically grown in the boreal region. This challenges the "effeciency hypothesis" that boreal crops may share the same acquisitive hydraulic strategy (i.e., high hydraulic efficiency) as those of the temperate and tropical regions measured in previous studies (Table S3).

On the other hand, our results support the "safety hypothesis" that the boreal climate may have imposed selective pressure on crops akin to that on wild plants, leading to a shared conservative hydraulic strategy in boreal crops, regardless of their distinct life forms. In line with the low hydraulic conductance, the hydraulic safety margin, as defined by the difference between the minimum leaf water potential experienced by the plant during its growth (ψ_{min}) and ψ_{50} (Choat et al., 2012; Anderegg et al., 2018), was found to be well above zero despite the large uncertainties in ψ_{50} (Fig. S9). This points to a high resistance of

https://doi.org/10.5194/egusphere-2025-5972
Preprint. Discussion started: 12 December 2025

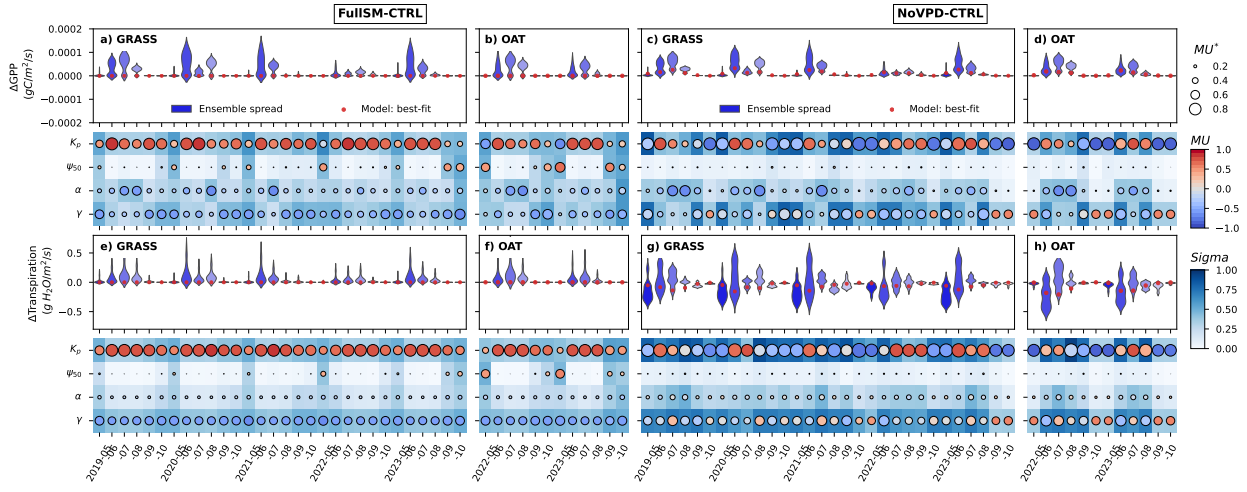

Figure 7. Modelled response of monthly averaged gross primary production (GPP) and transpiration to the absence of soil drought (FullSM-CTRL) (a, b, e, f) and atmospheric drought (NoVPD-CTRL) (c, d, g, h) at both the GRASS (a, c, e, g) and OAT (b, d, f, h) site. **FullSM**: QV_fullSM and HA_fullSM; **NoVPD**: QV_noVPD and HA_noVPD; **CTRL**: QV_ctrl and HA_ctrl. The upper panel of each subplot shows the spread of the ensemble experiments (violins), and the mean of the five best-fit PPE members (red dots). The lower panel of each subplot shows the Morris sensitivity of the simulated responses to the Phydro parameters (K_p, ψ_{50}, α, and γ).

the studied crops to the drought present in current climate conditions. We also demonstrate a low stomatal conductance (Fig. 8) and faster decline in leaf water potential than soil water potential, an indicator of anisohydric stomatal behaviour (Fig. S8a). Generally, stomatal closure occurs after significant loss of hydraulic conductivity (Fig. S9), implying a "risky" stomatal regulation and a low stomatal safety margin (Gleason et al., 2022; Martin-StPaul et al., 2017; Pereira et al., 2024). These are consistent with existing empirical evidence for perennial forage grasses (e.g. Holloway-Phillips and Brodribb, 2011b; Jacob et al., 2022) and some cereal crops (e.g. Corso et al., 2020).

The apparent hydraulic traits of both crops did not show large variations during the study periods (Fig. 3 and Methods S4), concurring that hydraulic traits are conserved features within species as noted by Lamy et al. (2014). There is only a weak plasticity of crop hydraulic traits seen in May, September, and October with wet and cool conditions, when different sets of Phydro parameters appear to fit slightly better to the observed fluxes (Methods S4). We also detected a slightly more acquisitive hydraulic strategy in the annual cereal crop (oat) and cover crop mix (annual ryegrass) than in the perennial forage grass (timothy, meadow fescue, white clover) (Table 1 and Fig. 3a–d), concurring with existing empirical studies (Table S3).

The low hydraulic efficiency was found to be critical for achieving a high GPP in summer when both soil and atmospheric drought were present, co-limiting crop productivity (Fig. 5). Such an effect, however, disappears when either soil or atmospheric drought is absent (Fig. S10 and S11). Under co-limiting conditions, crops with low hydraulic efficiency can better preserve soil moisture from being depleted to its critical threshold that significantly limits productivity (Fig. 5i, j and Fig. 6i, j), and thus maintain a higher productivity. This contradicts previous studies stressing the positive relation between hydraulic

https://doi.org/10.5194/egusphere-2025-5972
Preprint. Discussion started: 12 December 2025

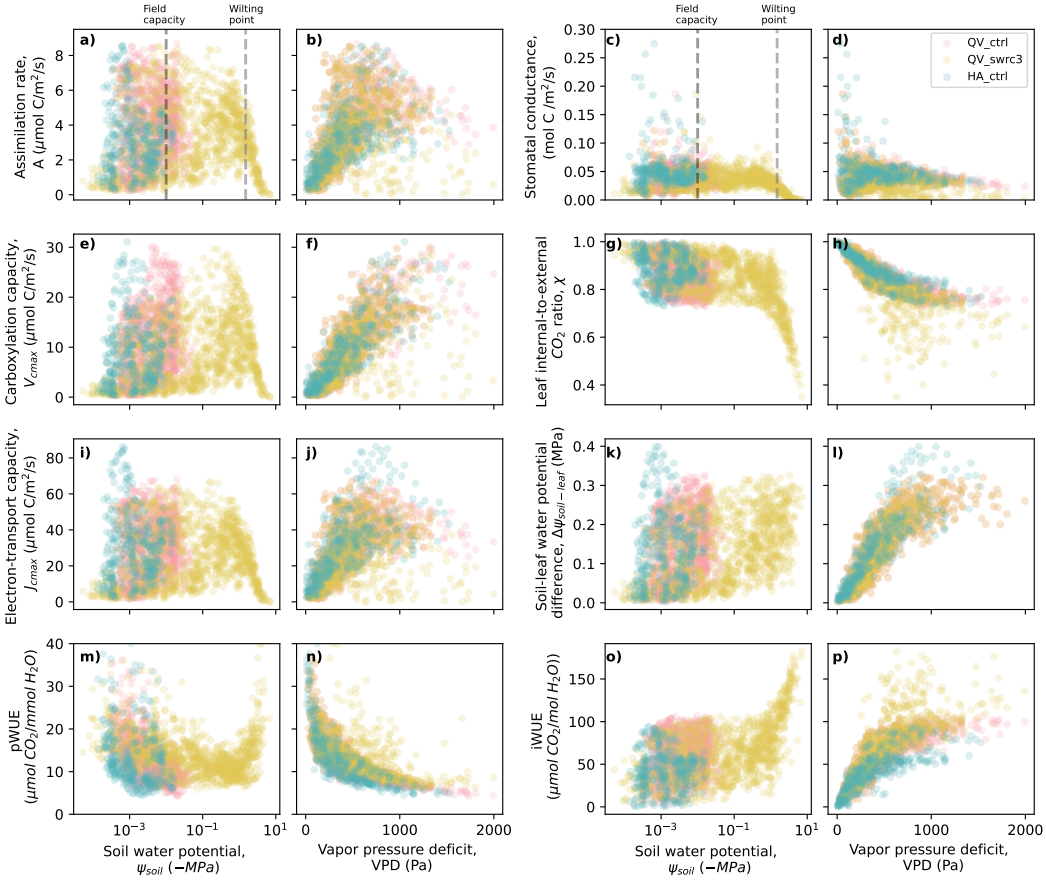

Figure 8. Daily response of photosynthetic and hydraulic variables to soil water potential (first and third column) and vapor pressure deficit (second and fourth column) simulated in the five best-fit PPE members selected from QV_ctrl, QV_swrc3, and HA_ctrl. (a,b) assimilation rate, (c,d) stomatal conductance, (e,f) leaf internal-to-external CO_2 ratio, (g,h) soil-leaf water potential difference, (i,j) Carboxylation capacity, (k,i) Electron-transport capacity, (m,n) plant-level water use efficiency (pWUE), (o,p) intrinsic water use efficiency (iWUE).

efficiency and GPP (Holloway-Phillips and Brodribb, 2011a; Ocheltree et al., 2016; Gleason et al., 2021), which is only visible during the cool and wet months in the early growing season (i.e., May) in our simulations (Fig. 6a, b). Our results, however, agree with the studies by Holloway-Phillips and Brodribb (2011a); Gleason et al. (2022), and Schell et al. (2025), which emphasise the critical role of conservative water use strategy in maintaining high crop yields during dry years.

Efforts have been made to find crops that can optimise both their GPP and pWUE in drought conditions (Leakey et al., 2019), but have rarely succeeded (Yu et al., 2020). Our results also show that crops may have optimised their GPP under drought conditions, but not necessarily pWUE (Fig. 5), which can be largely attributed to the contrasting impacts of hydraulic efficiency on GPP and pWUE (cf. Fig. 6a,b and e,f). There has been controversy over how plant hydraulic traits and their coordination affect pWUE. While high (low) hydraulic efficiency (safety) has often been suggested to promote pWUE (Holloway-Phillips

https://doi.org/10.5194/egusphere-2025-5972
Preprint. Discussion started: 12 December 2025

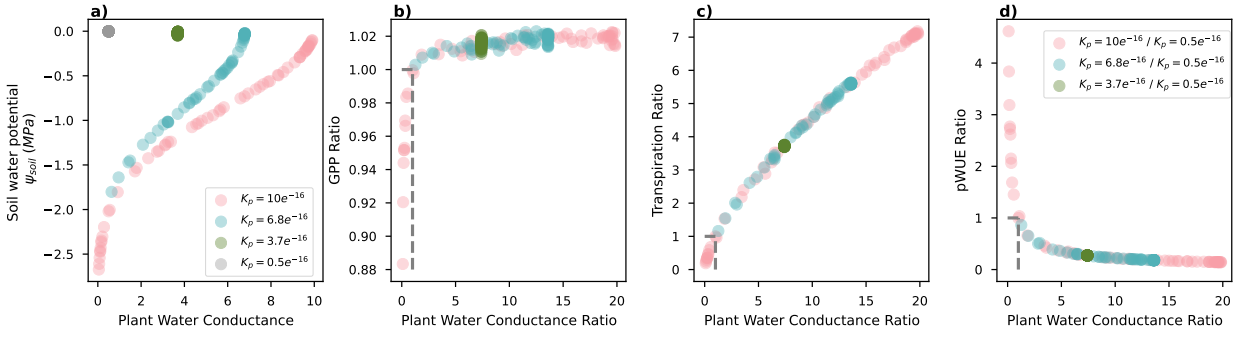

Figure 9. The relation between plant water conductance and soil water potential (a), the ratio of plant water conductance and the ratio of GPP (b), transpiration (c), and pWUE (d). The ratios were calculated between simulations with higher K_p and that with lowest K_p ($0.5e^{-16}$). They are all from QV_noVPD. The intersection of the horizontal and verticle grey dashlines in (b, c, d) denotes the reference point where the ratio equals to 1.

and Brodribb, 2011b; Gleason et al., 2022), low hydraulic efficiency has also been found to promote pWUE for alpine shrubs (Yao et al., 2024). Our modelling results do demonstrate a strong influence of hydraulic efficiency on pWUE under boreal conditions (Fig. 6e, f), but such impact is quite context dependent with positive (negative) effects in summer with water deficit (spring and autumn without water deficit). Similar effects are also observed in the empirical study on annual ryegrass (see Table 4 in Holloway-Phillips and Brodribb, 2011a).

We note that the positive impact of hydraulic efficiency on pWUE can arise particularly from the presence of soil drought (cf. Fig. S10 and S11). This can be explained by the fact that crop with high hydraulic efficiency can cause excessive soil water depletion, and thus lower soil and plant water potential more than a crop with low hydraulic efficiency (Fig. 9a). This can result in a significant decline of plant hydraulic conductance, which is shown to induce a negative effect on GPP and transpiration, but a positive effect on pWUE (Fig. 9b-d).

4.2 "Resistance" to soil drought, but not atmospheric drought

Our modelling results suggest a distinct response of boreal crops to soil and atmospheric drought (Fig. 7). We barely observed any soil drought stress on crop productivity in the simulations for both study sites unless a more drought-prone SWRC was used in the model (i.e., QV_swrc3) (Fig. 8). In contrast, the effects of VPD on productivity and WUE are well demonstrated at both study sites (Fig. 7c, d, g, h and 8). We hence argue that the extensive periods of high VPD may have been largely responsible for the reduction in yield during the drought years at the GRASS site reported by Heimsch et al. (2021). This supports the dominant role of atmospheric dryness in affecting productivity in the region (Mirabel et al., 2023), and helps to elucidate the high sensitivity of plant productivity to precipitation and cloud cover in the relatively "humid" boreal regions (Seddon et al., 2016).

https://doi.org/10.5194/egusphere-2025-5972
Preprint. Discussion started: 12 December 2025

The absence of soil water stress at both study sites is further confirmed by the analyses of critical soil moisture threshold proposed by Fu et al. (2024) (Fig. S8b-d). According to Fu et al. (2024), when soil moisture declines to a critical threshold, ecosystems can exhibit a sudden increase in the amplitude of the diurnal surface temperature and a decrease in the evaporative fraction (i.e., latent heat flux divided by absorbed solar radiation), signalling the onset of soil water stress on ecosystem functioning. We did not detect such a critical soil moisture threshold in both study sites using either flux measurements (Fig. S8c, d) or the model simulations. An exception is the simulation using a more drought-prone SWRC (QV_SWRC3), which displays a clear critical soil moisture threshold at 0.3 (Fig. S8b), overestimating soil drought stress at the site. We note that the above analyses do not include the potential impact of soil drought on the above- and below-ground carbon allocation of crops, which has been widely recognised in previous studies (Qiao et al., 2021; Xia et al., 2017). Whether such an effect was present at our study sites is worth further investigation, and a dynamic carbon allocation module considering the effects of soil drought would be needed for SPY-C to address this issue.

We also note that the lack of crop response to soil moisture changes (Fig. 7a,b)—often termed “resistance” to soil drought (Haugum et al., 2021)—was through "drought avoidance" mechanisms (Alves et al., 2024; Pereira et al., 2024; Cardoso et al., 2025), attributable to the low hydraulic efficiency of crops that prevents plants from depleting soil water too fast to the critical threshold (Fig. 5i,j and 6i,j). Low hydraulic efficiency also contributed in part to crop’s "resistance" to the atmopsheric drought (VPD), as evidenced by a positive impact of hydraulic conductance on the response of GPP to the absence of VPD in summer (Fig. 7c,d). However, this does not appear sufficient to fully relieve the stress of higher daily VPD (>=0.8 kPa), under which plant hydraulic coordination to sustain leaf water balance seems to be plateaued (Fig. 8i). As a result, both stomatal conductance and photosynthesis have to be reduced to inhibit excessive water loss from the leaves (Fig. 8b, d, f, g). A "risky" stomatal regulation with low stomatal safety margin exhibited in the studied crops (Fig. S9), however, did not show a clear association with their drought resistance, corroborating the recent finding on herbaceous crops by Pereira et al. (2024).

4.3 Model uncertainties and future development

Although the apparent hydraulic traits inferred from the best-fit parameter sets reproduced the observed fluxes across multiple temporal scales both within and beyond the calibration periods (Figs. 3 and 4) which underscores the fidelity of the approach, some discrepancies emerge when comparing our model inferences with empirical studies on similar temperate species (Fig. 10). In particular, the model suggests a lower K_p for perennial forage grass than previously reported leaf hydraulic conductance (Fig. 10d). Consequently, stomatal conductance is also underestimated, especially under high leaf water potential (Fig. 10a).

Given indications of potential overestimation of ET, especially the canopy and ground evaporation in SPY-C (Fig. 4b,d), we performed sensitivity experiments with reduced canopy and ground evaporation. However, the inferred K_p remained the same (data not shown), ruling out evaporation-related model biases as the primary source of such discrepancies. A more plausible explanation would be that the model inferred K_p reflects the whole-plant hydraulic conductance, which differs from leaf-level conductance typically measured in empirical studies. In addition, the measured species originate from temperate regions and represent different cultivars, which may exhibit traits distinct from boreal cultivars. Therefore, more empirical measurements on the hydraulic traits of Nordic crops are urgently needed to verify such conjectures.

https://doi.org/10.5194/egusphere-2025-5972
Preprint. Discussion started: 12 December 2025

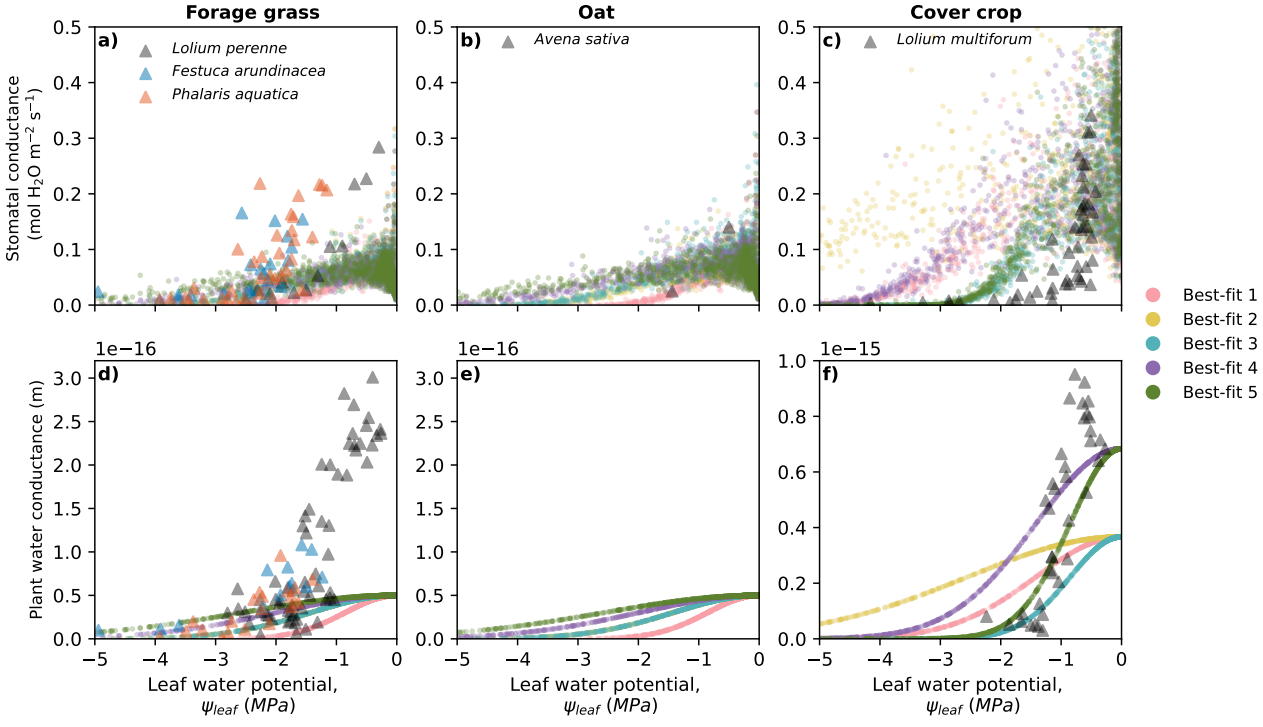

Figure 10. The modelled response of stomatal conductance (a-c) and leaf water conductance (d-f) to the decline of leaf water potential and their comparison with observed values of similar crops from literature. (a,d) are for forage grass, (b,e) are for oat and (c,f) are for cover crop. The modelled results from the five best-fit PPEs listed in Table 1 are denoted by circles. The empirical data are denoted by triangles, which are from Holloway-Phillips and Brodribb (2011b) (*Lolium perenne*), Jacob et al. (2022) (*Festuca arundinacea*, *Phalaris aquatica*), Canales et al. (2021) (*Avena sativa*) and Holloway-Phillips and Brodribb (2011a) (*Lolium multiforum*).

For oat and cover crop (annual ryegrass), the model generally captures the observed stomatal behaviour, except that annual ryegrass stomata tend to close more rapidly with dehydration (i.e., more isohydric) than the model predicts (Fig. 10b, c). High ψ_{50} (i.e., -1 MPa) seems to better reproduce the observed stomatal response to leaf dehydration. As values even higher than -1 MPa have recently been reported for some crops (Cardoso et al., 2025), increasing ψ_{50} above -1 MPa may further reduce the discrepancy between modelled and empirical results. Increasing the cost of maintaining hydraulic pathway (γ) can also induce more isohydric stomatal behaviour (data not shown). But again, empirical measurements on the hydraulic traits of boreal crops are prerequisite to verify the model-inferred hydraulic traits and resolve the mismatches shown in Fig. 10.

Despite uncertainties in absolute values, the importance of plant hydraulic traits in influencing boreal crop performance shown in this study underscores the necessity to implement plant hydraulic processes in crop models for better monitoring, reporting, and verifying (MRV) carbon balance in a crop field (Smith et al., 2020; Guan et al., 2023; Wijmer et al., 2024). SPY-C has shown good capability to simulate net ecosystem exchange (NEE) at the study sites (Fig. S12). To use SPY-C as a robust tool for MRV requires, for instance, more detailed representation of different crop managements. A nitrogen model coupled

https://doi.org/10.5194/egusphere-2025-5972
Preprint. Discussion started: 12 December 2025

with the carbon and water cycle (e.g. Stocker and Prentice, 2024) is also needed to better predict crop growth and carbon-water balance after fertilization. A larger scale of PPE covering the uncertainties of more parameters (e.g., soil hydrological parameters) and a more accurate and efficient benchmarking and inversion techniques (Denager et al., 2023; Bell et al., 2025) may also be implemented in the future to further improve its accuracy in retrieving crop hydraulic traits and simulating carbon and water balance at the crop field.

5 Conclusions

We examined the hydraulic traits of typical annual and perennial boreal crops and their impact on crop productivity, water use efficiency, and drought response, by leveraging carbon and water flux measurements from two Finnish crop fields and a newly developed SPY-C model equipped with coordinated photosynthetic and hydraulic processes. It is shown that both the annual cereal crop (oat) and the perennial forage grass exhibited a low apparent hydraulic efficiency and a conservative hydraulic strategy, which are crucial for dampening the impact of atmospheric drought and preventing soil water from being excessively depleted by crops during the growing season (drought avoidance), therefore maintaining both high crop productivity and drought resistance. Here, we present the newly developed SPY-C model as an efficient tool to assess crop hydraulic traits and their impact on crop performance in different pedoclimate conditions, which can be fundamental for selecting and developing better crops and managements to support climate-smart and sustainable agriculture. We also underscore the good potential of SPY-C for a wider application to monitoring, reporting, and verification framework to enhance their accuracy and predictive power in both current and future boreal climates.

Code and data availability. The meteorological and Sentinel-2 LAI data for Qvidja and Hauho sites are available from the Field Observatory website (https://www.fieldobservatory.org/) or from the Field Observatory dynamic data storage (Nevalainen et al., 2022b). The codes to retrieve Sentinel-2 satellite data and to calculate the leaf area index (LAI) are available from the Python satellitetools package (https://doi.org/10.5281/zenodo.5993291). Data for the gap-filled eddy covariance measurements are available at https://doi.org/10.57707/fmi-b2share.353cc686b81449d69117df30aeb3613c. The SPY-C model version used in this study is available at https://github.com/huitang-earth/SVMC/tree/v1.0.0. The model input and output are available at https://doi.org/10.57707/fmi-b2share.7536bc09eed44c71a08e87e545bc9406.

Author contributions. HT, SL, JV, LK, TP, JL designed the research. LK, HA, ON, MK, HV, JL collected observation data. HT, SL, JV, TP, IF, JPN, JL developed the SPY-C model. HT performed the research and data analysis. All the authors contribute to interpreting the results and writing the manuscript.

Competing interests. All authors declare no conflict of interest.

https://doi.org/10.5194/egusphere-2025-5972
Preprint. Discussion started: 12 December 2025

Acknowledgements. We thank Maria Tenkanen for helping improve the figures, Quentin Bell for inspiration about the model name and language checking, Laura Heimsch and Layla Höckerstedt for providing information of the study sites, Olli Niemitalo, Samu Varjonen and Iivari Kunttu for helpful discussions on the development of SPY-C. The authors wish to acknowledge CSC – IT Center for Science, Finland, for computational resources. ERA5-Land was downloaded from the Copernicus Climate Change Service (C3S). Neither the European Commission nor ECMWF is responsible for any use that may be made of the Copernicus information or data it contains.

Financial support. This work was supported by the Research Council of Finland (grant nos. 353073, 359342, 359533, 356138), the Strategic Research Council at the Research Council of Finland (grant no. 352431, 358257), the Ministry of Agriculture and Forestry of Finland (grant nos. VN/5094/2021 and VN/27979/2021), Business Finland (project 8391/31/2021), European Research Executive Agency (REA) through the Mission Soil project MARVIC (Grant Agreement: 101112942), Lantmännen Research Foundation and Lantmännen Group in Finland. In addition, this project has received funding from EU Horizon 2020 (grant no. 101056921).

https://doi.org/10.5194/egusphere-2025-5972
Preprint. Discussion started: 12 December 2025

References

Alves, RDFB., Menezes-Silva, PE., Loram-Lourenço, L., Abreu, IMPG., Alencar, KM., Sousa, LF., Almeida, SES., Aun, MA., Silva, MLF., Vasconcelos-Filho, SC., Silva, FG., Sales, JF., and Farnese, FS.: Exploring the Coordinated Hydraulic Plasticity across Organs in Soybean Plants Exposed to Drought Cycles, Environmental and Experimental Botany, 226, 105 871, https://doi.org/10.1016/j.envexpbot.2024.105871, 2024.

Anderegg, W. R. L., Klein, T., Bartlett, M., Sack, L., Pellegrini, A. F. A., Choat, B., and Jansen, S.: Meta-Analysis Reveals That Hydraulic Traits Explain Cross-Species Patterns of Drought-Induced Tree Mortality across the Globe, Proceedings of the National Academy of Sciences of the United States of America, 113, 5024–5029, https://doi.org/10.1073/pnas.1525678113, 2016.

Anderegg, W. R. L., Konings, A. G., Trugman, A. T., Yu, K., Bowling, D. R., Gabbitas, R., Karp, D. S., Pacala, S., Sperry, J. S., Sulman, B. N., and Zenes, N.: Hydraulic Diversity of Forests Regulates Ecosystem Resilience during Drought, Nature, 561, 538–541, https://doi.org/10.1038/s41586-018-0539-7, 2018.

Atkin, O. K., Bloomfield, K. J., Reich, P. B., Tjoelker, M. G., Asner, G. P., Bonal, D., Bönisch, G., Bradford, M. G., Cernusak, L. A., Cosio, E. G., Creek, D., Crous, K. Y., Domingues, T. F., Dukes, J. S., Egerton, J. J. G., Evans, J. R., Farquhar, G. D., Fyllas, N. M., Gauthier, P. P. G., Gloor, E., Gimeno, T. E., Griffin, K. L., Guerrieri, R., Heskel, M. A., Huntingford, C., Ishida, F. Y., Kattge, J., Lambers, H., Liddell, M. J., Lloyd, J., Lusk, C. H., Martin, R. E., Maksimov, A. P., Maximov, T. C., Malhi, Y., Medlyn, B. E., Meir, P., Mercado, L. M., Mirotchnick, N., Ng, D., Niinemets, Ü., O'Sullivan, O. S., Phillips, O. L., Poorter, L., Poot, P., Prentice, I. C., Salinas, N., Rowland, L. M., Ryan, M. G., Sitch, S., Slot, M., Smith, N. G., Turnbull, M. H., VanderWel, M. C., Valladares, F., Veneklaas, E. J., Weerasinghe, L. K., Wirth, C., Wright, I. J., Wythers, K. R., Xiang, J., Xiang, S., and Zaragoza-Castells, J.: Global Variability in Leaf Respiration in Relation to Climate, Plant Functional Types and Leaf Traits, New Phytologist, 206, 614–636, https://doi.org/10.1111/nph.13253, 2015.

Bell, Q., Gerin, S., Douglas, N., Quaife, T., Liski, J., and Viskari, T.: Calibrating Primary Crop Parameters to Capture Undersown Species Impacts, European Journal of Agronomy, 169, 127 676, https://doi.org/10.1016/j.eja.2025.127676, 2025.

Campolongo, F., Cariboni, J., and Saltelli, A.: An Effective Screening Design for Sensitivity Analysis of Large Models, Environmental Modelling & Software, 22, 1509–1518, https://doi.org/10.1016/j.envsoft.2006.10.004, 2007.

Canales, F. J., Rispail, N., García-Tejera, O., Arbona, V., Pérez-de-Luque, A., and Prats, E.: Drought Resistance in Oat Involves ABA-mediated Modulation of Transpiration and Root Hydraulic Conductivity, Environmental and Experimental Botany, 182, 104 333, https://doi.org/10.1016/j.envexpbot.2020.104333, 2021.

Cardoso, A. A., Andrade, M. T., Bucior, E. R., and Martins, S. C. V.: Plant Hydraulic Traits Influencing Crop Production in Water-Limited Environments, Plant Physiology, 199, https://doi.org/10.1093/plphys/kiaf521, 2025.

Choat, B., Jansen, S., Brodribb, T. J., Cochard, H., Delzon, S., Bhaskar, R., Bucci, S. J., Feild, T. S., Gleason, S. M., Hacke, U. G., Jacobsen, A. L., Lens, F., Maherali, H., Martínez-Vilalta, J., Mayr, S., Mencuccini, M., Mitchell, P. J., Nardini, A., Pittermann, J., Pratt, R. B., Sperry, J. S., Westoby, M., Wright, I. J., and Zanne, A. E.: Global Convergence in the Vulnerability of Forests to Drought, Nature, 491, 752–755, https://doi.org/10.1038/nature11688, 2012.

Corso, D., Delzon, S., Lamarque, L. J., Cochard, H., Torres-Ruiz, J. M., King, A., and Brodribb, T.: Neither Xylem Collapse, Cavitation, or Changing Leaf Conductance Drive Stomatal Closure in Wheat, Plant, Cell & Environment, 43, 854–865, https://doi.org/10.1111/pce.13722, 2020.

https://doi.org/10.5194/egusphere-2025-5972
Preprint. Discussion started: 12 December 2025

Denager, T., Sonnenborg, T. O., Looms, M. C., Bogena, H., and Jensen, K. H.: Point-Scale Multi-Objective Calibration of the Community Land Model (Version 5.0) Using in Situ Observations of Water and Energy Fluxes and Variables, Hydrology and Earth System Sciences, 27, 2827–2845, https://doi.org/10.5194/hess-27-2827-2023, 2023.

Fu, Z., Ciais, P., Wigneron, J.-P., Gentine, P., Feldman, A. F., Makowski, D., Viovy, N., Kemanian, A. R., Goll, D. S., Stoy, P. C., Prentice, I. C., Yakir, D., Liu, L., Ma, H., Li, X., Huang, Y., Yu, K., Zhu, P., Li, X., Zhu, Z., Lian, J., and Smith, W. K.: Global Critical Soil Moisture Thresholds of Plant Water Stress, Nature Communications, 15, 4826, https://doi.org/10.1038/s41467-024-49244-7, 2024.

Gan, Y., Duan, Q., Gong, W., Tong, C., Sun, Y., Chu, W., Ye, A., Miao, C., and Di, Z.: A Comprehensive Evaluation of Various Sensitivity Analysis Methods: A Case Study with a Hydrological Model, Environmental Modelling & Software, 51, 269–285, https://doi.org/10.1016/j.envsoft.2013.09.031, 2014.

Gerin, S., Vekuri, H., Liimatainen, M., Tuovinen, J.-P., Kekkonen, J., Kulmala, L., Laurila, T., Linkosalmi, M., Liski, J., Joki-Tokola, E., and Lohila, A.: Two Contrasting Years of Continuous N2O and CO2 Fluxes on a Shallow-Peated Drained Agricultural Boreal Peatland, Agricultural and Forest Meteorology, 341, 109 630, https://doi.org/10.1016/j.agrformet.2023.109630, 2023.

Gleason, S. M., Westoby, M., Jansen, S., Choat, B., Hacke, U. G., Pratt, R. B., Bhaskar, R., Brodribb, T. J., Bucci, S. J., Cao, K.-F., Cochard, H., Delzon, S., Domec, J.-C., Fan, Z.-X., Feild, T. S., Jacobsen, A. L., Johnson, D. M., Lens, F., Maherali, H., Martínez-Vilalta, J., Mayr, S., McCulloh, K. A., Mencuccini, M., Mitchell, P. J., Morris, H., Nardini, A., Pittermann, J., Plavcová, L., Schreiber, S. G., Sperry, J. S., Wright, I. J., and Zanne, A. E.: Weak Tradeoff between Xylem Safety and Xylem-Specific Hydraulic Efficiency across the World's Woody Plant Species, New Phytologist, 209, 123–136, https://doi.org/10.1111/nph.13646, 2016.

Gleason, S. M., Nalezny, L., Hunter, C., Bensen, R., Chintamanani, S., and Comas, L. H.: Growth and Grain Yield of Eight Maize Hybrids Are Aligned with Water Transport, Stomatal Conductance, and Photosynthesis in a Semi-Arid Irrigated System, Physiologia Plantarum, 172, 1941–1949, https://doi.org/10.1111/ppl.13400, 2021.

Gleason, S. M., Barnard, D. M., Green, T. R., Mackay, S., Wang, D. R., Ainsworth, E. A., Altenhofen, J., Brodribb, T. J., Cochard, H., Comas, L. H., Cooper, M., Creek, D., DeJonge, K. C., Delzon, S., Fritschi, F. B., Hammer, G., Hunter, C., Lombardozzi, D., Messina, C. D., Ocheltree, T., Stevens, B. M., Stewart, J. J., Vadez, V., Wenz, J., Wright, I. J., Yemoto, K., and Zhang, H.: Physiological Trait Networks Enhance Understanding of Crop Growth and Water Use in Contrasting Environments, Plant, Cell & Environment, 45, 2554–2572, https://doi.org/10.1111/pce.14382, 2022.

Guan, K., Jin, Z., Peng, B., Tang, J., DeLucia, E. H., West, P. C., Jiang, C., Wang, S., Kim, T., Zhou, W., Griffis, T., Liu, L., Yang, W. H., Qin, Z., Yang, Q., Margenot, A., Stuchiner, E. R., Kumar, V., Bernacchi, C., Coppess, J., Novick, K. A., Gerber, J., Jahn, M., Khanna, M., Lee, D., Chen, Z., and Yang, S.-J.: A Scalable Framework for Quantifying Field-Level Agricultural Carbon Outcomes, Earth-Science Reviews, 243, 104 462, https://doi.org/10.1016/j.earscirev.2023.104462, 2023.

Haddix, M. L., Gregorich, E. G., Helgason, B. L., Janzen, H., Ellert, B. H., and Francesca Cotrufo, M.: Climate, Carbon Content, and Soil Texture Control the Independent Formation and Persistence of Particulate and Mineral-Associated Organic Matter in Soil, Geoderma, 363, 114 160, https://doi.org/10.1016/j.geoderma.2019.114160, 2020.

Haugum, S. V., Thorvaldsen, P., Vandvik, V., and Velle, L. G.: Coastal Heathland Vegetation Is Surprisingly Resistant to Experimental Drought across Successional Stages and Latitude, Oikos, 130, 2015–2027, https://doi.org/10.1111/oik.08098, 2021.

Heimsch, L., Lohila, A., Tuovinen, J.-P., Vekuri, H., Heinonsalo, J., Nevalainen, O., Korkiakoski, M., Liski, J., Laurila, T., and Kulmala, L.: Carbon Dioxide Fluxes and Carbon Balance of an Agricultural Grassland in Southern Finland, Biogeosciences, 18, 3467–3483, https://doi.org/10.5194/bg-18-3467-2021, 2021.

https://doi.org/10.5194/egusphere-2025-5972
Preprint. Discussion started: 12 December 2025

Heimsch, L., Vira, J., Fer, I., Vekuri, H., Tuovinen, J.-P., Lohila, A., Liski, J., and Kulmala, L.: Impact of Weather and Management Practices on Greenhouse Gas Flux Dynamics on an Agricultural Grassland in Southern Finland, Agriculture, Ecosystems & Environment, 374, 109 179, https://doi.org/10.1016/j.agee.2024.109179, 2024.

Henry, C., John, G. P., Pan, R., Bartlett, M. K., Fletcher, L. R., Scoffoni, C., and Sack, L.: A Stomatal Safety-Efficiency Trade-off Constrains Responses to Leaf Dehydration, Nature Communications, 10, 3398, https://doi.org/10.1038/s41467-019-11006-1, 2019.

Herman, J. and Usher, W.: SALib: An Open-Source Python Library for Sensitivity Analysis, Journal of Open Source Software, 2, 97, https://doi.org/10.21105/joss.00097, 2017.

Holloway-Phillips, M.-M. and Brodribb, T. J.: Contrasting Hydraulic Regulation in Closely Related Forage Grasses: Implications for Plant Water Use, Functional Plant Biology, 38, 594–605, https://doi.org/10.1071/FP11029, 2011a.

Holloway-Phillips, M.-M. and Brodribb, T. J.: Minimum Hydraulic Safety Leads to Maximum Water-Use Efficiency in a Forage Grass, Plant, Cell & Environment, 34, 302–313, https://doi.org/10.1111/j.1365-3040.2010.02244.x, 2011b.

Huo, J., Shi, Y., Chen, J., Zhang, H., Feng, L., Zhao, Y., and Zhang, Z.: Hydraulic Trade-off and Coordination Strategies Mediated by Leaf Functional Traits of Desert Shrubs, Frontiers in Plant Science, 13, https://doi.org/10.3389/fpls.2022.938758, 2022.

Jacob, V., Choat, B., Churchill, A. C., Zhang, H., Barton, C. V. M., Krishnananthaselvan, A., Post, A. K., Power, S. A., Medlyn, B. E., and Tissue, D. T.: High Safety Margins to Drought-Induced Hydraulic Failure Found in Five Pasture Grasses, Plant, Cell & Environment, 45, 1631–1646, https://doi.org/10.1111/pce.14318, 2022.

Joshi, J., Stocker, B. D., Hofhansl, F., Zhou, S., Dieckmann, U., and Prentice, I. C.: Towards a Unified Theory of Plant Photosynthesis and Hydraulics, Nature Plants, 8, 1304–1316, https://doi.org/10.1038/s41477-022-01244-5, 2022.

Kennedy, D., Swenson, S., Oleson, K. W., Lawrence, D. M., Fisher, R., Lola da Costa, A. C., and Gentine, P.: Implementing Plant Hydraulics in the Community Land Model, Version 5, Journal of Advances in Modeling Earth Systems, 11, 485–513, https://doi.org/10.1029/2018MS001500, 2019.

Lamarque, L. J., Delzon, S., Toups, H., Gravel, A.-I., Corso, D., Badel, E., Burlett, R., Charrier, G., Cochard, H., Jansen, S., King, A., Torres-Ruiz, J. M., Pouzoulet, J., Cramer, G. R., Thompson, A. J., and Gambetta, G. A.: Over-Accumulation of Abscisic Acid in Transgenic Tomato Plants Increases the Risk of Hydraulic Failure, Plant, Cell & Environment, 43, 548–562, https://doi.org/10.1111/pce.13703, 2020.

Lamy, J.-B., Delzon, S., Bouche, P. S., Alia, R., Vendramin, G. G., Cochard, H., and Plomion, C.: Limited Genetic Variability and Phenotypic Plasticity Detected for Cavitation Resistance in a Mediterranean Pine, New Phytologist, 201, 874–886, https://doi.org/10.1111/nph.12556, 2014.

Launiainen, S., Guan, M., Salmivaara, A., and Kieloaho, A.-J.: Modeling Boreal Forest Evapotranspiration and Water Balance at Stand and Catchment Scales: A Spatial Approach, Hydrology and Earth System Sciences, 23, 3457–3480, https://doi.org/10.5194/hess-23-3457-2019, 2019.

Launiainen, S., Kieloaho, A.-J., Lindroos, A.-J., Salmivaara, A., Ilvesniemi, H., and Heiskanen, J.: Water Retention Characteristics of Mineral Forest Soils in Finland: Impacts for Modeling Soil Moisture, Forests, 13, 1797, https://doi.org/10.3390/f13111797, 2022.

Leakey, A. D. B., Ferguson, J. N., Pignon, C. P., Wu, A., Jin, Z., Hammer, G. L., and Lobell, D. B.: Water Use Efficiency as a Constraint and Target for Improving the Resilience and Productivity of C3 and C4 Crops, Annual Review of Plant Biology, 70, 781–808, https://doi.org/10.1146/annurev-arplant-042817-040305, 2019.

Li, S., Wang, J., Lu, S., Salmon, Y., Liu, P., and Guo, J.: Trade-Off between Hydraulic Safety and Efficiency in Plant Xylem and Its Influencing Factors, Forests, 14, 1817, https://doi.org/10.3390/f14091817, 2023.

https://doi.org/10.5194/egusphere-2025-5972
Preprint. Discussion started: 12 December 2025

Liu, H., Taylor, S. H., Xu, Q., Lin, Y., Hou, H., Wu, G., and Ye, Q.: Life History Is a Key Factor Explaining Functional Trait Diversity among Subtropical Grasses, and Its Influence Differs between C3 and C4 Species, Journal of Experimental Botany, 70, 1567–1580, https://doi.org/10.1093/jxb/ery462, 2019.

Liu, H., Ye, Q., Gleason, S. M., He, P., and Yin, D.: Weak Tradeoff between Xylem Hydraulic Efficiency and Safety: Climatic Seasonality Matters, New Phytologist, 229, 1440–1452, https://doi.org/10.1111/nph.16940, 2021a.

Liu, H., Ye, Q., Lundgren, M. R., Young, S. N. R., Liu, X., Luo, Q., Lin, Y., Ye, N., and Hao, G.: Phylogeny and Climate Explain Contrasting Hydraulic Traits in Different Life Forms of 150 Woody Fabaceae Species, Journal of Ecology, 112, 741–754, https://doi.org/10.1111/1365-2745.14266, 2024.

Liu, Y., Kumar, M., Katul, G. G., Feng, X., and Konings, A. G.: Plant Hydraulics Accentuates the Effect of Atmospheric Moisture Stress on Transpiration, Nature Climate Change, 10, 691–695, https://doi.org/10.1038/s41558-020-0781-5, 2020.

Liu, Y., Holtzman, N. M., and Konings, A. G.: Global Ecosystem-Scale Plant Hydraulic Traits Retrieved Using Model–Data Fusion, Hydrology and Earth System Sciences, 25, 2399–2417, https://doi.org/10.5194/hess-25-2399-2021, 2021b.

Lloyd, J. and Taylor, J. A.: On the Temperature Dependence of Soil Respiration, Functional Ecology, 8, 315–323, https://doi.org/10.2307/2389824, 1994.

Lu, Y., Sloan, B., Thompson, S. E., Konings, A. G., Bohrer, G., Matheny, A., and Feng, X.: Intra-Specific Variability in Plant Hydraulic Parameters Inferred From Model Inversion of Sap Flux Data, Journal of Geophysical Research: Biogeosciences, 127, e2021JG006777, https://doi.org/10.1029/2021JG006777, 2022.

Martin-StPaul, N., Delzon, S., and Cochard, H.: Plant Resistance to Drought Depends on Timely Stomatal Closure, Ecology Letters, 20, 1437–1447, https://doi.org/10.1111/ele.12851, 2017.

Mirabel, A., Girardin, M. P., Metsaranta, J., Way, D., and Reich, P. B.: Increasing Atmospheric Dryness Reduces Boreal Forest Tree Growth, Nature Communications, 14, 6901, https://doi.org/10.1038/s41467-023-42466-1, 2023.

Morales, J. L. and Nocedal, J.: Remark on "Algorithm 778: L-BFGS-B: Fortran Subroutines for Large-Scale Bound Constrained Optimization", ACM Trans. Math. Softw., 38, 7:1–7:4, https://doi.org/10.1145/2049662.2049669, 2011.

Morris, M. D.: Factorial Sampling Plans for Preliminary Computational Experiments, Technometrics, 33, 161–174, https://doi.org/10.1080/00401706.1991.10484804, 1991.

Muñoz-Sabater, J., Dutra, E., Agustí-Panareda, A., Albergel, C., Arduini, G., Balsamo, G., Boussetta, S., Choulga, M., Harrigan, S., Hersbach, H., Martens, B., Miralles, D. G., Piles, M., Rodríguez-Fernández, N. J., Zsoter, E., Buontempo, C., and Thépaut, J.-N.: ERA5-Land: A State-of-the-Art Global Reanalysis Dataset for Land Applications, Earth System Science Data, 13, 4349–4383, https://doi.org/10.5194/essd-13-4349-2021, 2021.

Nevalainen, O., Niemitalo, O., Fer, I., Juntunen, A., Mattila, T., Koskela, O., Kukkamäki, J., Höckerstedt, L., Mäkelä, L., Jarva, P., Heimsch, L., Vekuri, H., Kulmala, L., Stam, Å., Kuusela, O., Gerin, S., Viskari, T., Vira, J., Hyväluoma, J., Tuovinen, J.-P., Lohila, A., Laurila, T., Heinonsalo, J., Aalto, T., Kunttu, I., and Liski, J.: Towards Agricultural Soil Carbon Monitoring, Reporting, and Verification through the Field Observatory Network (FiON), Geoscientific Instrumentation, Methods and Data Systems, 11, 93–109, https://doi.org/10.5194/gi-11-93-2022, 2022a.

Nevalainen, O., Niemitalo, O., Fer, I., Juntunen, A., Mattila, T., Koskela, O., Kukkamäki, J., Höckerstedt, L., Mäkelä, L., Jarva, P., Heimsch, L., Vekuri, H., Kulmala, L., Stam, Å., Kuusela, O., Gerin, S., Viskari, T., Vira, J., Hyväluoma, J., Tuovinen, J.-P., Lohila, A., Laurila, T., Heinonsalo, J., Aalto, T., Kunttu, I., and Liski, J.: Field Observatory Dynamic Data Storage, https://doi.org/10.23728/fmi-b2share.56513f096ca442b19abdef30f63644ed, 2022b.

https://doi.org/10.5194/egusphere-2025-5972
Preprint. Discussion started: 12 December 2025

Ocheltree, T. W., Nippert, J. B., and Prasad, P. V. V.: A Safety vs Efficiency Trade-off Identified in the Hydraulic Pathway of Grass Leaves Is Decoupled from Photosynthesis, Stomatal Conductance and Precipitation, New Phytologist, 210, 97–107, https://doi.org/10.1111/nph.13781, 2016.

Palosuo, T., Heikkinen, J., and Regina, K.: Method for Estimating Soil Carbon Stock Changes in Finnish Mineral Cropland and Grassland Soils, Carbon Management, 6, 207–220, https://doi.org/10.1080/17583004.2015.1131383, 2015.

Pereira, T. S., Oliveira, L. A., Andrade, M. T., Haverroth, E. J., Cardoso, A. A., and Martins, S. C. V.: Linking Water-Use Strategies with Drought Resistance across Herbaceous Crops, Physiologia Plantarum, 176, e14 114, https://doi.org/10.1111/ppl.14114, 2024.

Poque, S., Carlson-Nilsson, U., Omer, M., Himanen, K., and Khazaei, H.: Exploring an Automated Indoor High-Throughput Phenotyping Facility to Investigate the Response of Faba Bean to Water Stress, https://doi.org/10.21203/rs.3.rs-6461902/v1, 2025.

Pritzkow, C., Williamson, V., Szota, C., Trouvé, R., and Arndt, S. K.: Phenotypic Plasticity and Genetic Adaptation of Functional Traits Influences Intra-Specific Variation in Hydraulic Efficiency and Safety, Tree Physiology, 40, 215–229, https://doi.org/10.1093/treephys/tpz121, 2020.

Qiao, S., Wang, H., Prentice, I. C., and Harrison, S. P.: Optimality-Based Modelling of Climate Impacts on Global Potential Wheat Yield, Environmental Research Letters, 16, 114 013, https://doi.org/10.1088/1748-9326/ac2e38, 2021.

Ramírez-Valiente, J. A., Poyatos, R., Blackman, C. J., Cabon, A., Castells, E., Cochard, H., Creek, D., Delzon, S., García-Valdés, R., Limousin, J.-M., López, R., Martin-StPaul, N., Moreno, M., Rowland, L., Santiago, L. S., Schuldt, B., Torres-Ruiz, J. M., Valade, A., Martínez-Vilalta, J., and Mencuccini, M.: Limited Plastic Responses in Safety Traits Support Greater Hydraulic Risk under Drier Conditions, Nature Ecology & Evolution, pp. 1–12, https://doi.org/10.1038/s41559-025-02830-4, 2025.

Rantanen, M., Kämäräinen, M., Niittynen, P., Phoenix, G. K., Lenoir, J., Maclean, I., Luoto, M., and Aalto, J.: Bioclimatic Atlas of the Terrestrial Arctic, Scientific Data, 10, 40, https://doi.org/10.1038/s41597-023-01959-w, 2023.

Reichstein, M., Falge, E., Baldocchi, D., Papale, D., Aubinet, M., Berbigier, P., Bernhofer, C., Buchmann, N., Gilmanov, T., Granier, A., Grünwald, T., Havránková, K., Ilvesniemi, H., Janous, D., Knohl, A., Laurila, T., Lohila, A., Loustau, D., Matteucci, G., Meyers, T., Miglietta, F., Ourcival, J.-M., Pumpanen, J., Rambal, S., Rotenberg, E., Sanz, M., Tenhunen, J., Seufert, G., Vaccari, F., Vesala, T., Yakir, D., and Valentini, R.: On the Separation of Net Ecosystem Exchange into Assimilation and Ecosystem Respiration: Review and Improved Algorithm, Global Change Biology, 11, 1424–1439, https://doi.org/10.1111/j.1365-2486.2005.001002.x, 2005.

Roitsch, T., Himanen, K., Chawade, A., Jaakola, L., Nehe, A., and Alexandersson, E.: Functional Phenomics for Improved Climate Resilience in Nordic Agriculture, Journal of Experimental Botany, 73, 5111–5127, https://doi.org/10.1093/jxb/erac246, 2022.

Sanchez-Martinez, P., Martínez-Vilalta, J., Dexter, K. G., Segovia, R. A., and Mencuccini, M.: Adaptation and Coordinated Evolution of Plant Hydraulic Traits, Ecology Letters, 23, 1599–1610, https://doi.org/10.1111/ele.13584, 2020.

Schaap, M. G. and Van Genuchten, M. T.: A Modified Mualem–van Genuchten Formulation for Improved Description of the Hydraulic Conductivity Near Saturation, Vadose Zone Journal, 5, 27–34, https://doi.org/10.2136/vzj2005.0005, 2006.

Schell, V., Kervroëdan, L., Corso, D., N'do, D. Y., Faucon, M.-P., and Delzon, S.: Greater Resistance to Drought-Induced Embolism Is Linked to Higher Yield Maintenance in Soybean, Plant, Cell & Environment, https://doi.org/10.1111/pce.15538, 2025.

Seddon, A. W. R., Macias-Fauria, M., Long, P. R., Benz, D., and Willis, K. J.: Sensitivity of Global Terrestrial Ecosystems to Climate Variability, Nature, 531, 229–232, https://doi.org/10.1038/nature16986, 2016.

Sierra, C. A., Ceballos-Núñez, V., Hartmann, H., Herrera-Ramírez, D., and Metzler, H.: Ideas and Perspectives: Allocation of Carbon from Net Primary Production in Models Is Inconsistent with Observations of the Age of Respired Carbon, Biogeosciences, 19, 3727–3738, https://doi.org/10.5194/bg-19-3727-2022, 2022.

https://doi.org/10.5194/egusphere-2025-5972
Preprint. Discussion started: 12 December 2025

Smith, P., Soussana, J.-F., Angers, D., Schipper, L., Chenu, C., Rasse, D. P., Batjes, N. H., van Egmond, F., McNeill, S., Kuhnert, M., Arias-Navarro, C., Olesen, J. E., Chirinda, N., Fornara, D., Wollenberg, E., Álvaro-Fuentes, J., Sanz-Cobena, A., and Klumpp, K.: How to Measure, Report and Verify Soil Carbon Change to Realize the Potential of Soil Carbon Sequestration for Atmospheric Greenhouse Gas Removal, Global Change Biology, 26, 219–241, https://doi.org/10.1111/gcb.14815, 2020.

Sperry, J. S. and Love, D. M.: What Plant Hydraulics Can Tell Us about Responses to Climate-Change Droughts, New Phytologist, 207, 14–27, https://doi.org/10.1111/nph.13354, 2015.

Spinoni, J., Vogt, J. V., Naumann, G., Barbosa, P., and Dosio, A.: Will Drought Events Become More Frequent and Severe in Europe?, International Journal of Climatology, 38, 1718–1736, https://doi.org/10.1002/joc.5291, 2018.

Stocker, B. D. and Prentice, I. C.: CN-model: A Dynamic Model for the Coupled Carbon and Nitrogen Cycles in Terrestrial Ecosystems, https://doi.org/10.1101/2024.04.25.591063, 2024.

Sun, Q., Gilgen, A. K., Signarbieux, C., Klaus, V. H., and Buchmann, N.: Cropping Systems Alter Hydraulic Traits of Barley but Not Pea Grown in Mixture, Plant, Cell & Environment, 44, 2912–2924, https://doi.org/10.1111/pce.14054, 2021.

Torres-Ruiz, J. M., Cochard, H., Delzon, S., Boivin, T., Burlett, R., Cailleret, M., Corso, D., Delmas, C. E. L., De Caceres, M., Diaz-Espejo, A., Fernández-Conradi, P., Guillemot, J., Lamarque, L. J., Limousin, J.-M., Mantova, M., Mencuccini, M., Morin, X., Pimont, F., De Dios, V. R., Ruffault, J., Trueba, S., and Martin-StPaul, N. K.: Plant Hydraulics at the Heart of Plant, Crops and Ecosystem Functions in the Face of Climate Change, New Phytologist, 241, 984–999, https://doi.org/10.1111/nph.19463, 2024.

Vekuri, H., Tuovinen, J.-P., Kulmala, L., Papale, D., Kolari, P., Aurela, M., Laurila, T., Liski, J., and Lohila, A.: A Widely-Used Eddy Covariance Gap-Filling Method Creates Systematic Bias in Carbon Balance Estimates, Scientific Reports, 13, 1–9, https://doi.org/10.1038/s41598-023-28827-2, 2023.

Vico, G. and Brunsell, N. A.: Tradeoffs between Water Requirements and Yield Stability in Annual vs. Perennial Crops, Advances in Water Resources, 112, 189–202, https://doi.org/10.1016/j.advwatres.2017.12.014, 2018.

Vira, J., Vekuri, H., Nevalainen, O., Korkiakoski, M., Mattila, T., Aaltonen, H., Koskinen, M., Lohila, A., Pihlatie, M., and Liski, J.: Improving Agricultural Carbon Monitoring with Sentinel-2 and Eddy-Covariance-Based Plant Productivity Estimates, Carbon Management, 16, 2568 042, https://doi.org/10.1080/17583004.2025.2568042, 2025.

Viskari, T., Pusa, J., Fer, I., Repo, A., Vira, J., and Liski, J.: Calibrating the Soil Organic Carbon Model Yasso20 with Multiple Datasets, Geoscientific Model Development, 15, 1735–1752, https://doi.org/10.5194/gmd-15-1735-2022, 2022.

Wang, D. R., Venturas, M. D., Mackay, D. S., Hunsaker, D. J., Thorp, K. R., Gore, M. A., and Pauli, D.: Use of Hydraulic Traits for Modeling Genotype-specific Acclimation in Cotton under Drought, New Phytologist, 228, 898–909, https://doi.org/10.1111/nph.16751, 2020.

Wang, S., Li, J., Yu, P., Guo, L., Zhou, J., Yang, J., and Wu, W.: Convergent Evolution in Angiosperms Adapted to Cold Climates, Plant Communications, 6, 101 258, https://doi.org/10.1016/j.xplc.2025.101258, 2025.

Weiss, M., Baret, F., and Jay, S.: S2 Toolbox Level 2 Product Algorithms, Tech. rep., European Space Agency, 2020.

Wijmer, T., Al Bitar, A., Arnaud, L., Fieuzal, R., and Ceschia, E.: AgriCarbon-EO v1.0.1: Large-Scale and High-Resolution Simulation of Carbon Fluxes by Assimilation of Sentinel-2 and Landsat-8 Reflectances Using a Bayesian Approach, Geoscientific Model Development, 17, 997–1021, https://doi.org/10.5194/gmd-17-997-2024, 2024.

Xia, J., Yuan, W., Wang, Y.-P., and Zhang, Q.: Adaptive Carbon Allocation by Plants Enhances the Terrestrial Carbon Sink, Scientific Reports, 7, 3341, https://doi.org/10.1038/s41598-017-03574-3, 2017.

https://doi.org/10.5194/egusphere-2025-5972
Preprint. Discussion started: 12 December 2025

Yao, G.-Q., Nie, Z.-F., Zeng, Y.-Y., Waseem, M., Hasan, M. M., Tian, X.-Q., Liao, Z.-Q., Siddique, K. H. M., and Fang, X.-W.: A Clear Trade-off between Leaf Hydraulic Efficiency and Safety in an Aridland Shrub during Regrowth, Plant, Cell & Environment, 44, 3347–3357, https://doi.org/10.1111/pce.14156, 2021.

Yao, G.-Q., Qi, S.-H., Li, Y.-R., Duan, Y.-N., Jiang, C., Nie, Z.-F., Liu, X.-D., Hasan, M. M., Xu, D.-H., Jing, W.-M., McAdam, S., and Fang, X.-W.: The Combination of High Leaf Hydraulic Safety and Water Use Efficiency Allows Alpine Shrubs to Adapt to High-Altitude Habitats, Functional Ecology, 38, 2506–2517, https://doi.org/10.1111/1365-2435.14660, 2024.

Yu, L., Gao, X., and Zhao, X.: Global Synthesis of the Impact of Droughts on Crops' Water-Use Efficiency (WUE): Towards Both High WUE and Productivity, Agricultural Systems, 177, 102 723, https://doi.org/10.1016/j.agsy.2019.102723, 2020.

Zhao, Q., Chen, J., Kang, J., and Kang, S.: Trade-Offs Between Hydraulic Efficiency and Safety in Cotton (Gossypium Hirsutum L.) Stems Under Elevated CO2 and Salt Stress, Plants, 14, 298, https://doi.org/10.3390/plants14020298, 2025.